remote sensing

MDPI

Article

Global Distribution and Morphodynamic Patterns of Paired Spits Developed at the Mouths of Interdistributary Bays of Deltas and within Coastal Channels

Javier Alcántara-Carrió [1,*], Ángela Fontán-Bouzas [2,3], Ana Caicedo Rodríguez [4], Rogério Portantiolo Manzolli [1] and Luana Portz [1]

[1] Department of Geology and Geochemistry, Faculty of Sciences, Autonomous University of Madrid, C/Tomás y Valiente 7, 29049 Madrid, Spain; rogerio.manzolli@uam.es (R.P.M.); luana.portz@uam.es (L.P.)
[2] Department of Geodynamics, Stratigraphy and Paleontology, Faculty of Geological Sciences, Complutense University of Madrid, C/José Antonio Novais 12, 28040 Madrid, Spain; anfontan@ucm.es
[3] CIM–UVIGO GEOMA, University of Vigo, 36310 Vigo, Spain
[4] Seccional Oceanografía, Universidad of Antioquia, C/104 #110-2a, Cra. 25 #110120, Turbo 057867, Colombia; ana.caicedo@udea.edu.co
* Correspondence: javier.alcantara@uam.es

Abstract: Previously, paired spits have been described at the mouths of bays, estuaries, and deltas. This study analyzed the worldwide distribution and morphodynamic patterns of paired spits located at the mouths of interdistributary bays of deltas (three systems) and within coastal channels (24 systems). The methodology was based on the detailed analysis of satellite images, nautical charts, and tidal-range databases. The paired spits found were mainly located on microtidal coasts at high or mid latitudes. Waves were the main factor controlling convergent progradation and breaching of the spits, while the hydraulic blockage for the development of these paired spits was mainly due to tide-induced currents, as well as minor fluvial outlets in the interdistributary bays. Three morphodynamic patterns were identified: (i) stable, with low progradation rates, generally without breaching or degradation of any of the spits; (ii) stationary, with high progradation rates, alternating degradation or breaching of any of the spits with the formation of new spits or closure of the breaches; and (iii) instable or ephemeral, which included three subtypes, the severe erosion of one or both spits, the joining of the head of the two spits forming a single barrier, and the merging of each with its channel margin.

Keywords: geomorphology; baymouth spits; double spits; progradation; erosion; degradation; breaching

Citation: Alcántara-Carrió, J.; Fontán-Bouzas, Á.; Caicedo Rodríguez, A.; Manzolli, R.P.; Portz, L. Global Distribution and Morphodynamic Patterns of Paired Spits Developed at the Mouths of Interdistributary Bays of Deltas and within Coastal Channels. *Remote Sens.* **2023**, *15*, 2713. https://doi.org/10.3390/rs15112713

Received: 14 April 2023
Revised: 18 May 2023
Accepted: 19 May 2023
Published: 23 May 2023

1. Introduction

Sandy and gravel spits are elongated barriers that extend laterally through the successive construction of progradational beach ridges [1–3]. Wave-induced processes are the main factor controlling spit development [4]. Bays and estuaries are often partially enclosed by spits [5]. Intense littoral drift leads to the formation of spits in the outer parts of the bays, which can evolve into systems of sand bars and coastal lagoons, with a mouth maintained by tidal currents or rivers flowing into the bay [6,7]. Similarly, littoral drift also forms barrier spits at estuarine river mouths, which can break up due to intense river discharge events [8–11], storms [12–14], tsunami events [15], the temporal decrease of sediment supply [16] or artificial breaching [17]. Spits also develop in asymmetric and very asymmetric (deflected) wave-dominated deltas [18–21], where they can be extremely dynamic [22].

On exceptional occasions, the bays, estuaries, and deltas are confined by systems of paired spits (PS), i.e., two spits with a converging longshore drift that partially or almost completely enclose the bay or river mouth. The formation of paired spits has been described by five morphogenetic models: (i) coastal barrier break [23,24]; (ii) convergent longshore

drift in a narrow bay [25]; (iii) bidirectional longshore drift with hydraulic blockage [26]; (iv) cutting a detached spit due to ebb-tidal currents [27] or by high energy events such as storms [28], hurricanes [29] or high fluvial discharge [30]; and (v) the convergence of two estuary mouths and the associated spits [30]. In previous studies about paired spits, they are also referred to as baymouth spits, double spits or baymouth barriers. The term paired spits is also used for gravel or sandy points growing within coastal lagoons [31], with countless examples worldwide [32–36].

The formation and evolution of convergent baymouth spits is influenced by the hydrodynamics of waves, tides, and river discharge. In narrow bays, the convergent progradation of both spits may be due to unidirectional frontal waves, which generate a convergent littoral drift from both ends of the bay [25]. On the other hand, on open coasts, the paired convergent spits are related to a seasonal alternation of bidirectional waves. At each time of the year, the waves favor the development of one of the spits, while the hydraulic blockage, generated by tidal currents [29,37] or intense fluvial discharge [27,30,38], favors the net progradation of the countercurrent spit, by preventing or at least minimizing its erosion by the dominant waves. Usually, paired spits have been described at the mouth of bays and rivers [39]. However, the development of paired spits constraining the mouths of interdistributary bays of deltas has only been described for the Po River delta (N Adriatic Sea) [40–44], and the development of paired spits within channels have only been very briefly reported [45–47]. Therefore, determining the global distribution, geomorphological characteristics and morphodynamic evolution of paired spits located both at the interdistributary bays of deltas and within coastal channels was the main objective of this study.

2. Materials and Methods

The analysis of open mean resolution of satellite LANDSAT imagery with worldwide and five-decades historical coverage, supported by high performance platforms such as Google Earth Pro, is a very useful tool to investigate coastal processes, such as shoreline changes [48–50] and spit morphodynamics [12,38,51] on a planetary scale and in an economical way. The identification of the global distribution and a description of the four-decades geomorphological evolution of all the paired spits in the world found at the mouths of interdistributary bays of deltas and within coastal channels were obtained by analyzing annual series of LANDSAT satellite imagery (1984–2020), supported by Google Earth™ [52]. Exceptionally, for a small system within the Safaga Strait (NW Red Sea), data were analyzed using Satellite Quickbird imagery, with a higher spatial resolution; data were only available since 2003 in Google Earth Pro. This platform does not provide access to the original multispectral data and therefore a supervised shoreline extraction could not be realized.

Initially, the shoreline of each spit was digitized using the Google Earth ruler tool. The traced lines can be considered as representations of the mean littoral zone because tidal variations are not taken into account in these images [53]. However, monitoring the length of the shoreline from the root to the head is not useful when determining spit progradation, because this length also increases due to small cuspate forelands, beach cusps or local erosion, for instance at the neck of the spit. Therefore, a reference line was defined joining the root of the two spits, along the axis of each spit up to the head (considering the head of the spit for each year to follow its progradation), passing through the inlet between the heads and following the longitudinal axis of the possible islands (Figure 1). This reference line was defined following [29], but it is not straight now, because the morphology and head progradation of the spits are not straight either. The 1984–2020 evolution of the distance, on this reference line, from the root to the head of the spits, as well as to the ends of the developed islands, were measured using the Google Earth ruler tool.

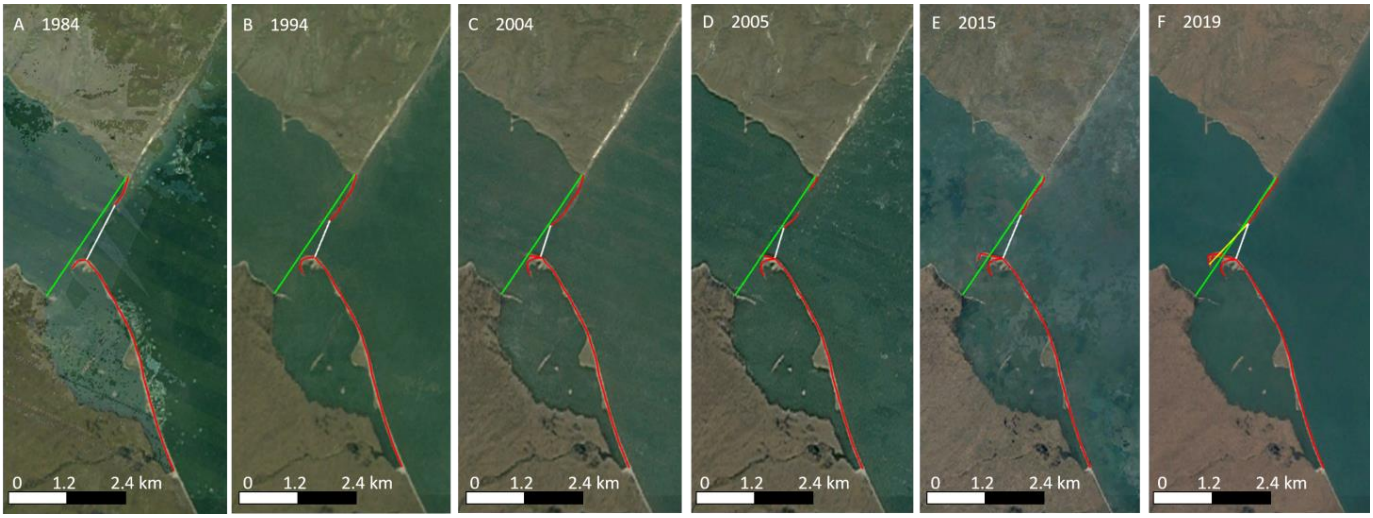

Figure 1. Plot and measurement of annual axial lines (red lines) from the root to the head of each spit for the period from 1984 (**A**) to 2020. The length of successive hooked ridges (**B**,**E**) was measured in order to determine head progradation, but not the changes in neck curvature (**C**). Formation of islands by spit breaching (**D**) and the new formation of spits (**D**–**F**) were also monitored. The reference line considers the longest axial line for each spit and the distance (yellow line) between the heads of the two spits (**F**). The minimum width of the inlet (white line) varied from year to year, but the width at the entrance of the channel or at the mouth of the interdistributary bay (green line) was considered constant throughout the study period.

The distances obtained were plotted using Grapher™ (Golden Software) and the head progradation rates (m/yr) for the spits were determined on these graphs. In the case of spit degradation, such as on the western margin of the Scardovari lagoon and on the eastern margin of the Goro lagoon (both in the SW sector of the Po River delta), they were monitored using the old spit before its partial degradation as the new spit that developed afterwards.

The long-term scale decrease in width, due to constriction by the development of paired spits, was defined as the ratio of the length of the main inlet to the length of the original mouth of the interdistributary bay or of the original entrance to the channel without considering the paired spits. The minimum width of the main inlet was measured on the digitized shorelines of the spits, varying over the study period 1984–2020. The width of the original baymouth or the channel entrance, which was considered constant for the study period, was measured directly from satellite imagery.

The maximum depth of the inlet between the two spits, for each paired spits system, was determined by analysis of online bathymetric charts supported by Navionics® Chart Viewer [54], except for the Goro lagoon, which was obtained from [55]. Bathymetric data supported by Google Earth, based on the bathymetric model of [56] and its updates, were initially considered but later discarded, due to inconsistencies between these data and both the nautical charts and the spits morphology observed in the satellite images.

The offshore data series near each paired spits system of the mean wave direction, peak period (Tp) and significant height (Hs) of combined wind, waves, and swell were obtained from the ERA5 reanalysis [57] for the period 2018–2021 (except for PS-17 which were for the period 2010–2013). For each data series, the percentage of the year with data (i.e., a proxy for the period free of ice sheet formation at high latitudes) was calculated, and directional histograms (wave roses) were plotted by Grapher™ (Golden Software) to identify the uni-, bi- or multi-directional wave regimes. Then, for the first and second significant directions identified considering the wave approach and coastal orientation, the mean annual and 95% percentile of Hs (m), and the predominance of wind sea (Tp < 6 s), swell (Tp > 9 s) or intermediate peak periods (6 to 9 s) were determined. Offshore wave propagation by numerical models was not carried out because high-resolution bathymetry

is not available for many of the study sites, due to the fact that they are located in remote areas and have very dynamic systems, and therefore bathymetric charts are not accurate. Satellite-derived bathymetry can help solve this problem for future detailed research of each study area, even though it also has limitations, such as turbidity or the short window of opportunity for many of them due to ice-sheet formation [58].

Tidal range (m) was obtained using the free online software WXTIDE [59], except for the paired spits located in Canada, where it was replaced by data available online from the tidal data stations supported by the Canadian Hydrographic Service [60]. Each paired spits system was then classified as micro- (0–2), meso- (2–4), macro- (4–6) or mega-tidal (>6 m), according to criteria of [61,62]. The development of ice plates at high-latitude coastal areas, which impedes the morphodynamic evolution of the paired spits, was confirmed by observation of monthly LANDSAT-8 satellite imagery, supported by the USGS GloVis online repository [63].

The presence of local human activities was obtained from the analysis of satellite images and then cross-checked with bibliographic information. The spits were classified as natural, rural, semi-urban, urban, or artificial coasts following [64]. The rural coast included agricultural uses and small harbors for fishing activities, as well as spits on natural coast with the presence of coastal defense structures.

In summary, the methodology applied in this study included: the extraction of the shoreline of the paired spits by analyzing satellite images; the determination of the geomorphological characteristics of the spits; the plotting of the evolution of the head of the spits and the ends of the islands; the calculation of both the rates of head progradation and the decrease in width at the mouth of the interdistributary delta bays or at the entrance to the channels; the determination of the maximum inlet depth and the tidal range for each system; the description of morphodynamic events (spit breaching, development of spit islands, closure of breaches, degradation of spits, and formation of new spits); the analysis of hydrodynamic control, sediment availability and sedimentary interactions; the definition of morphogenetic models and natural morphodynamic patterns; and the analysis of human disturbances. It is summarized in the workflow (Figure 2).

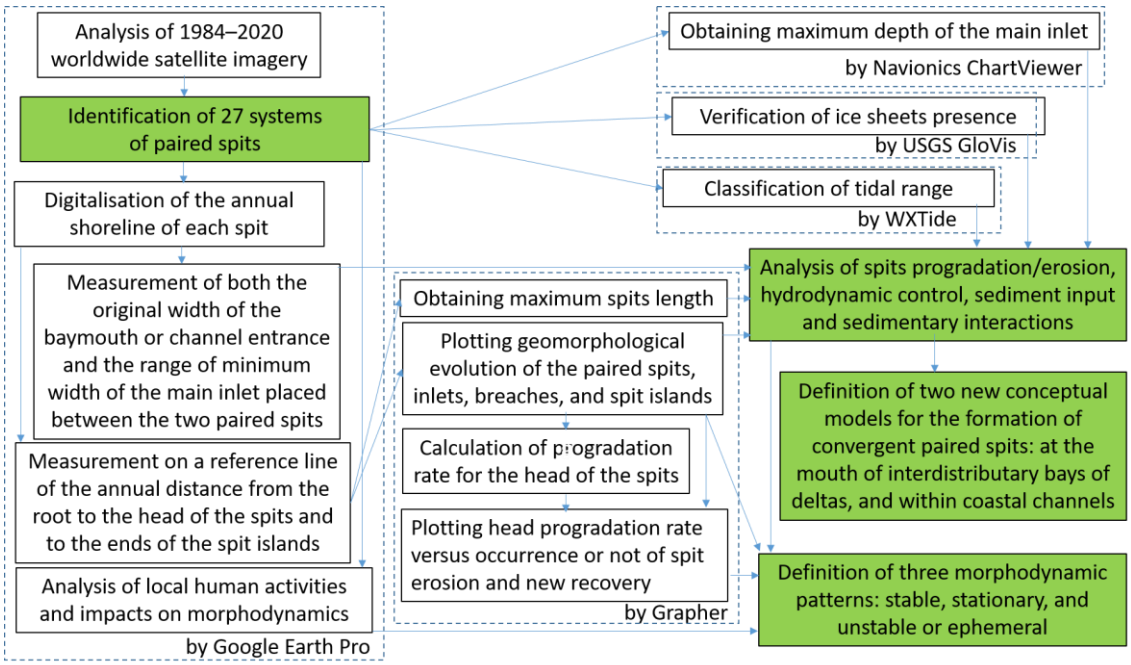

Figure 2. Workflow. The main results are indicated in green boxes.

3. Results

3.1. Global Distribution and Geomorphological Description

Twenty-seven systems of paired spits at the mouth of interdistributary bays of deltas and within coastal channels were identified (Figures 3 and 4). They are mainly located on microtidal coasts of high or mid latitudes, although they have also been found on mesotidal coasts and at low latitudes (Table 1). All of them were found in the northern hemisphere, except for one ephemeral system located on the southwest coast of Angola (PS-27). Three paired spits systems were identified at the mouths of interdistributary bays of deltas. PS-1 is located at the mouth of Demarcation Bay (South of the Beaufort Sea), an interdistributary bay between the Kongakut and Clarence River deltas. The western spit of PS-1 developed from the barrier island off the Kongakut River delta, and the eastern spit is a barrier spit developed from the Clarence River delta. PS-2 and PS3, are located, respectively, at the mouth of the Scardovari and Goro lagoons, in two interdistributary bays of the Po River delta,. The other twenty-four paired spits systems were identified at the entrance to coastal channels, except for: PS-24, which is in the middle of the Safaga Strait (Red Sea); PS-10 in the middle of the Litke Strait, between Karaginsky Island and the Kamchatka Peninsula (Bering Sea); and PS-17 in the northern sector within the Strait of Canso (Northeastern of the Nova Scotia Peninsula) (Table 1). PS-6 is located at the entrance to the channel between Booth and Fiji Islands (South of the Beaufort Sea), and there is another spit in the northern margin, within the channel. Similarly, eastward of PS-7 (West of the Parry Peninsula, South of the Beaufort Sea), the nautical chart shows that there was also a second spit within the channel, on the northern margin, but satellite imagery showed that it was almost completely degraded before 1985. Another particular coastal configuration are channels with paired spits at both entrances, which is the case for PS-12 and PS-13 in the Tugidak Passage, between Tugidak and Sitkinak islands (West of Gulf of Alaska), and PS-25 and PS-26 in Almejas Bay, between Santa Margarita Island and the western coast of Baja California Peninsula. In addition, three entrances to Nantucket Sound (Northwest Atlantic Ocean) are limited by the development of paired spits, one of them between Monomoy and Nantucket islands (PS-20), and two others in the Muskeget Channel (PS-21 between Tuckernuck and Muskeget islands, and PS-22 between Nantucket and Tuckernuck islands).

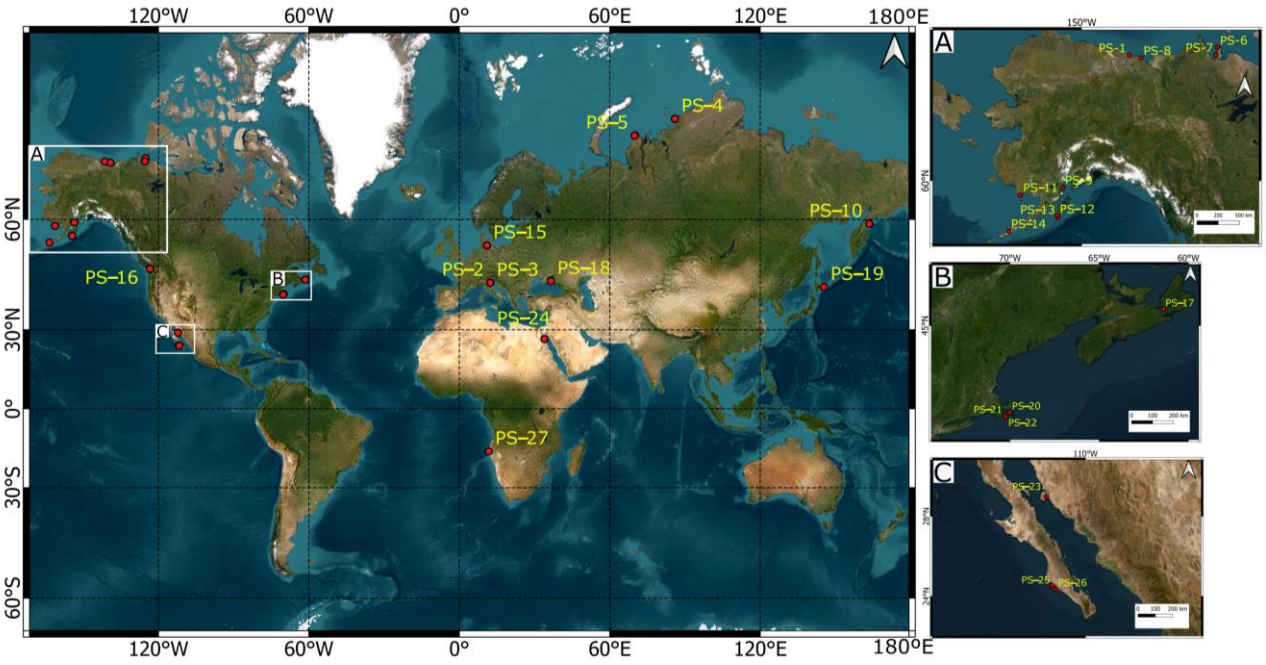

Figure 3. Global distribution of paired spits at the mouths of interdistributary bays of deltas (PS-1 to PS-3) and within coastal channels (PS-4 to PS-27). Detailed locations are shown for (**A**) NW North America, (**B**) E North America, and (**C**) SW North America.

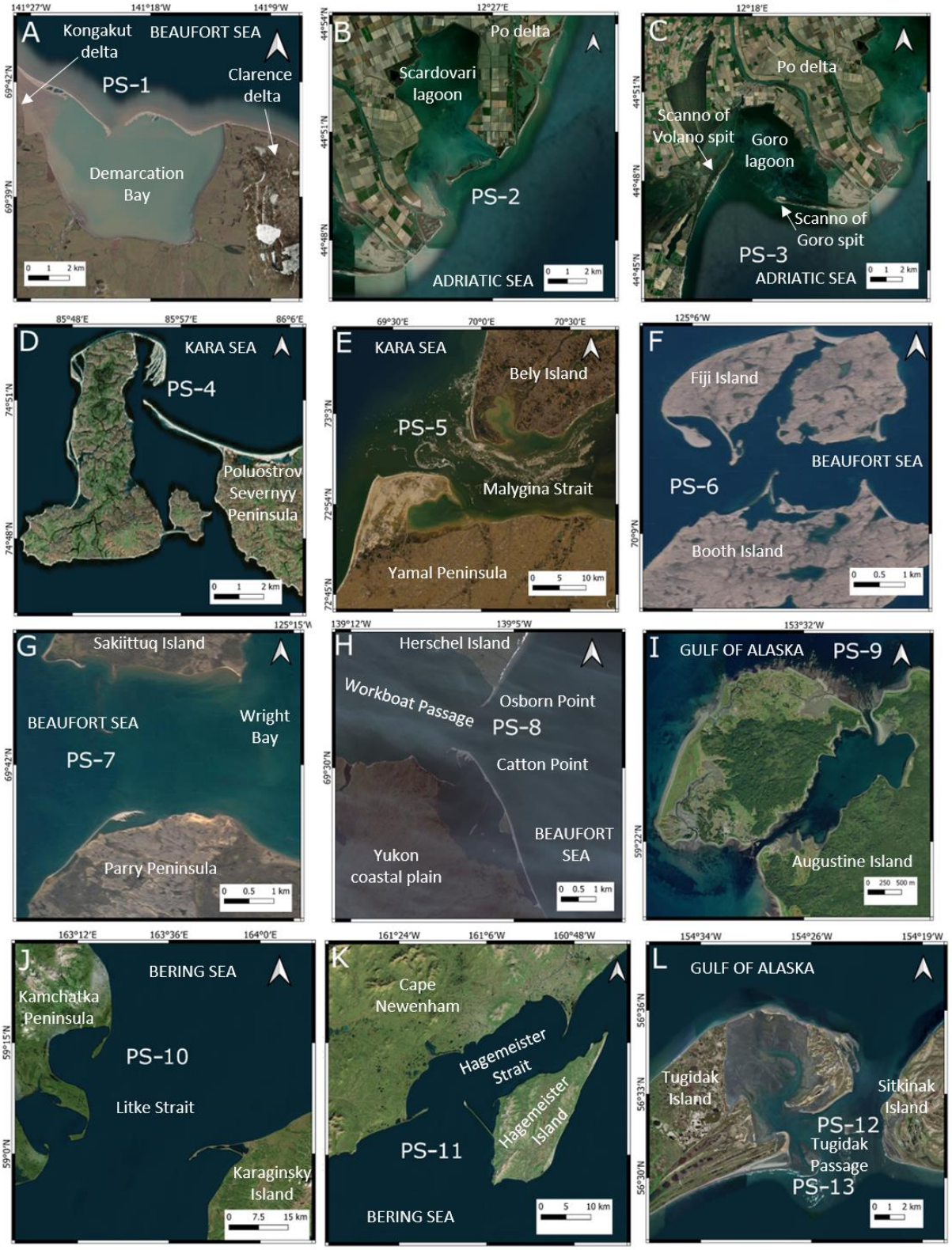

Figure 4. *Cont.*

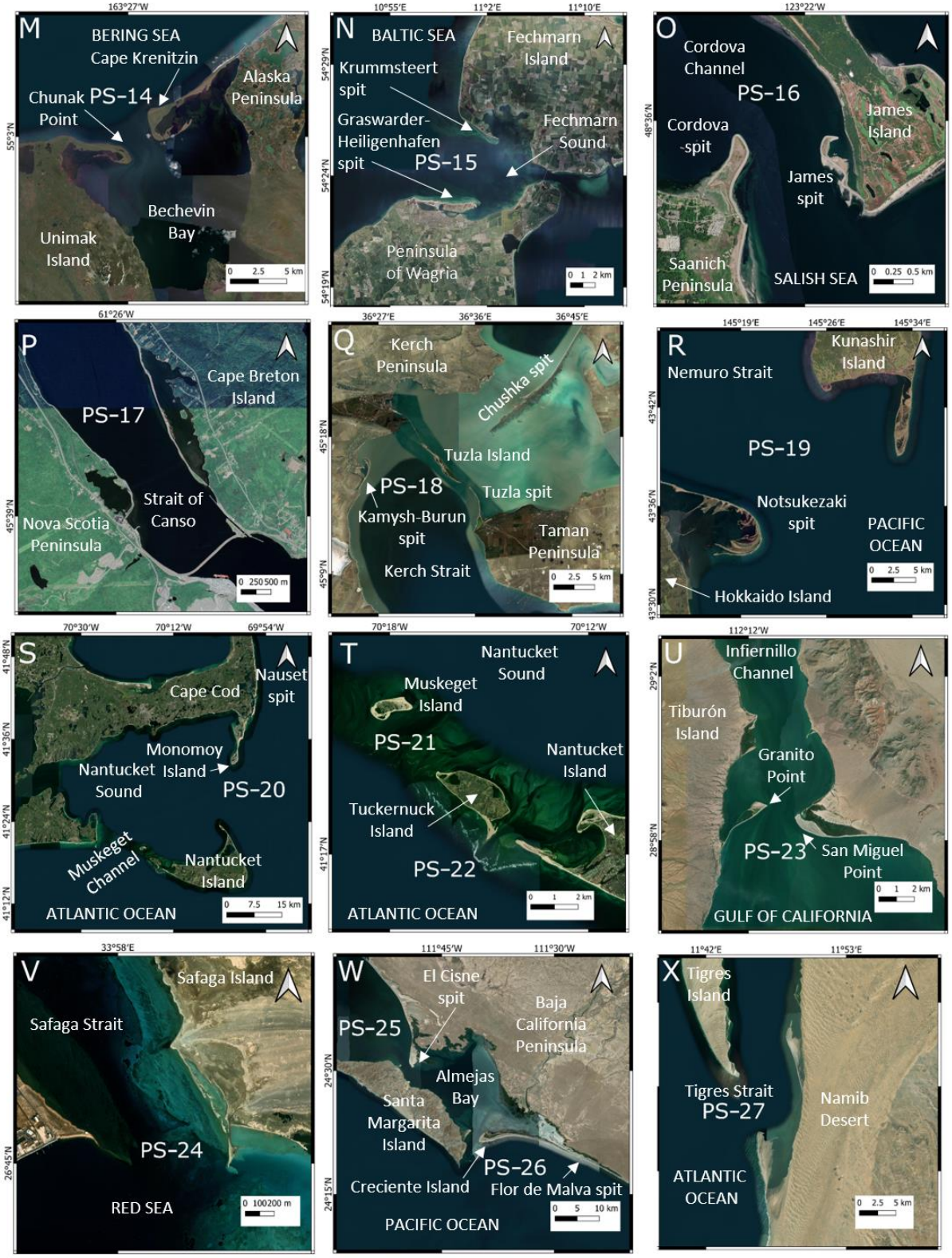

Figure 4. Paired spits (PS) located at the mouths of interdistributary bays of deltas (PS-1 to PS-3) and within coastal channels (PS-4 to PS-27). (Source of the images: ESRI Satellite, Google Satellite, and Bing Satellite). (**A**) PS-1, (**B**) PS-2, (**C**) PS-3, (**D**) PS-4, (**E**) PS-5, (**F**) PS-6, (**G**) PS-7, (**H**) PS-8, (**I**) PS-9, (**J**) PS-10, (**K**) PS-11, (**L**) PS-12 and PS-13, (**M**) PS-14, (**N**) PS-15, (**O**) PS-16, (**P**) PS-17, (**Q**) PS-18, (**R**) PS-19, (**S**) PS-20, (**T**) PS-21 and PS-22, (**U**) PS-23, (**V**) PS-24, (**W**) PS-25 and PS-26, (**X**) PS-27.

Table 1. Location, tidal range, and morphological characteristics (1984–2020) of the paired spits identified at the mouth of the interdistributary bays of deltas (PS-1 to PS-3) and within coastal channels (PS-4 to PS-27). Their morphology of the paired spits is parameterized by the maximum length (m) of the longest and the shortest spit, the ratio between them, the maximum depth (m) of the inlet between the head of both spits, and the decrease in width, i.e., the ratio of the width of the main inlet to the original width of the mouth of the interdistributary bay or channel.

Paired Spits	Latitude	Longitude	Place	Region	Tidal Range	Longest Spit	Shortest Spit	Length Ratio	Inlet Depth	Width Decrease
PS-1	69.68°N	141.34°W	Demarcation Bay	Beaufort Sea	micro–	5965	5647	1.06	5.2	0.02–0.14
PS-2	44.82°N	12.43°E	Scardovari lagoon	Adriatic Sea	micro–	2393	2188	1.09	2.2	0.21–0.41
PS-3	44.80°N	12.30°E	Goro lagoon		micro–	8313	6741	1.23	3.5	0.17–0.42
PS-4	74.84°N	85.95°E	NW Poluostrov Severnyy Peninsula	Kara Sea	micro–	3978	3460	1.15	<5	0.05–0.18
PS-5	72.98°N	69.92°E	Malygina Strait		micro–	31,329	6466	4.85	<5	0.35
PS-6	70.16°N	125.07°W	Channel between Booth and Fiji islands	Beaufort Sea	micro–	1181	379	3.12	13.5	0.40
PS-7	69.70°N	125.36°W	W of Parry Peninsula		micro–	2435	361	6.75	0.3	0.71–0.72
PS-8	69.51°N	139.11°W	Workboat Passage		micro–	5626	1472	3.82	6.4	0.19–0.44
PS-9	59.38°N	153.52°W	Augustine Island	Gulf of Alaska	meso–	487	182	2.68	0.3	0.33
PS-10	59.10°N	163.50°E	Litke Strait	Bering Sea	micro–	16,831	9272	1.82	5	0.77
PS-11	58.68°N	161.23°W	Hagemeister Strait		meso–	8990	5131	1.75	20.1	0.42
PS-12	56.58°N	154.49°W	Tugidak Passage	Gulf of Alaska	meso–	17,941	2326	7.71	31	0.15–0.16
PS-13	56.52°N	154.40°W			meso–	15,934	5780	2.77	31	0.289
PS-14	55.05°N	163.44°W	NW Bechevin Bay	Bering Sea	micro–	11,860	6119	1.94	23.8	0.17
PS-15	54.41°N	10.99°E	Fehmarn Sound	Baltic Sea	micro–	4931	2624	1.88	12.3	0.74–0.75
PS-16	48.59°N	123.36°W	Cordova Channel	Salish Sea	meso–	1177	1083	1.09	32	0.62
PS-17	45.65°N	61.43°W	Strait of Canso	Gulf of St. Lawrence	micro–	2640	582	4.53	40	0.58
PS-18	45.24°N	36.54°E	Kerch Strait	Black Sea	micro–	4795	2186	2.19	6.7	0.46
PS-19	43.61°N	145.44°E	Nemuro Strait	Sea of Okhotsk	micro–	24,613	1810	13.60	20	0.68
PS-20	41.47°N	70.03°W	Main Channel	Nantucket Sound, NW Atlantic Ocean	micro–	15,443	8282	1.86	17.0	0.46–0.47
PS-21	41.32°N	70.29°W	Muskeget Channel		micro–	2047	887	2.31	1.2	0.72–1
PS-22	41.28°N	70.24°W			micro–	2765	1444	1.91	7.3	0.53–0.67
PS-23	28.97°N	112.18°W	Infiernillo Channel	Gulf of California	micro–	4797	3585	1.34	13.4	0.19
PS-24	26.75°N	33.96°E	Safaga Strait	Red Sea	micro–	887	340	2.61	0.5	0.59–0.89
PS-25	24.51°N	111.83°W	Almejas Bay	NE Pacific Ocean	micro–	15,231	1149	13.25	26.6	0.09–0.10
PS-26	24.37°N	111.67°W			micro–	11,408	3339	10.66	13.2	0.08
PS-27	16.73°S	11.75°E	Tigres Strait	SE Atlantic Ocean	micro–	15,346	2961	5.18	9.7	———

The maximum length along the shore of the spits, from root to head, ranges from 31,359 m for the southern spit of PS-5 in the Malygina Strait, which separates Bely Island from the Yamal Peninsula (Northwest of Siberia), to 182 m for the western spit of PS-9, located in a small channel cutting through the volcanic Augustine Island (West of Gulf of Alaska). The maximum length of both spits is similar in the interdistributary bays, but the length of the longest spit within channels varies from the same order to more than thirteen times the length of the shortest spit (Table 1).

The formation of paired spits reduces the width at the mouth of the interdistributary bays or channels. Maximum closure is identified for PS-1, in Demarcation Bay, and for PS-4,

in a channel between Tsirkul Island and the Poluostrov Severnyy Peninsula (E Kara Sea), remaining around 2–5% of the original width. It was not possible to determine the decrease in width for PS-27 because the width of the channel progressively increased due to high erosion at the southern end of the Tigres island.

The maximum depth between the head of the paired spits ranges from less than 1 m to 40 m (Table 1). In some systems, the local depth increases significantly just between the two spits, along the entire inlet, as is the case on the Hagemeister Strait (PS-11), the Tugidak Passage (PS-12, PS-13), and the Infiernillo Channel (PS-23), or only right next to one of the spits, as is the case of the eastern spit of PS-14 in the NW entrance to Bechevin Bay, and the Notsukezaki spit (PS-19), in the western margin of the southern entrance to the Nemuro Strait.

3.2. Natural Morphodynamics

Most of the paired spits are very dynamic, with high progradation rates reaching up to 156.93 m/yr (PS-20). In some paired spits, the longest spits show higher progradation rates that the shortest ones, but in others, the opposite is true. Progradation in some recurved spits is not identified from the head, but from the middle of the spit, allowing new hooked ridges to develop. The eastern recurved spit of PS-19 shows progradation from the middle and the head of the spit. In contrast, other paired spits show very low progradation rates, which cannot be measured due to the resolution of the satellite images used, without other significant geomorphological changes; these progradation rates must be lower than 1 m/yr, i.e., below the detection threshold of the analysis carried out (Table 2). The the migration of some of the spits from the surrounding coast to the mouth of the channel (northern spit of PS-20), or alongside of the channel towards the central sector (southern spit of PS-7, western spit of PS-22, eastern spit of PS-24, and western spit of PS-25), has been observed, as well as a rotation of the spits from the root (both spits of PS-21, western spits of PS-24 and PS-26).

Progradation is usually combined with erosion, which results in the degradation or breaching of some of the spits, developing minor inlets and spit islands. Subsequently, some of these spit islands eroded completely (PS-3, PS-8), but in other cases the breaches closed, and they joined the previous spit (PS-22, PS-25), or continued as islands by their natural evolution (PS-26) or because the limits of the spit islands and the head of the spit was fixed by coastal defense structures (PS-2; PS-18). It is also possible that the spit islands migrated to the mainland, developing new spits (PS-20). Extreme erosion due to the development of new inlets reaches a shoreline retreat of up to −167.65 m/yr, for the head of the northern spit of PS-27, and has even led to total degradation of one of the spits (northern spit of PS-20, western spit of PS-21, and northern spit of PS-27) or severe root retreat of the northern spit of PS-27 (Figure 5). Cannibalization of the root of the western spit of PS-12 was also identified, while coastal defenses were built close to the root of other spits (e.g., the southern spit of PS-15, the two spits of PS-17, western spit of PS-19) to avoid their erosion.

The development of the paired spits constrains the interdistributary bay or channel (Figure 4; Table 1). Positive progradation rates of the spits were observed in the study period (Table 2) as well as a decrease in the width of the main inlet (Figure 5), although in several cases, this decrease was very small compared to the overall dimensions of the system (PS-20, PS-26). However, in one exceptional case (PS-24), there was an increase in the width of the main inlet, due to the 40° clockwise rotation of the western spit, i.e., towards its channel margin. At PS-27, similar rates of progradation of the southern spit and erosion of the northern spit (Table 2) resulted in a northward migration of the inlet with a slight increase in its width (Figure 5L). The main inlet of PS-22 also showed a westward migration, combined with an alternately decreasing, increasing, and again decreasing width (Figure 5I).

Table 2. Natural morphodynamic processes of the paired spits located at the mouths of interdistributary bays of deltas (PS-1 to PS-3) and within coastal channels (PS-4 to PS-27): average progradation rate (m/yr; negative values for erosion), presence of hooked ridges, breaching of the spit developing a spit island or degradation of the spit by erosion, merging of the island with the rest of the spit or formation of a new spit, and classification of the natural morphodynamic pattern.

Paired Spits	Progradation Rate			Hooked Ridges	Spit Breaching or Degradation	Spits Merging or Formation of a New Spit	Morphodynamic Pattern
	Study Period	Longer Spit	Shorter Spit				
PS-1	1984–2020	10.88	16.83	Yes	Yes	Yes	Ephemeral
PS-2	1984–1989	104.54	106.88	Yes	Yes	Yes	Stationary
PS-3	1984–2020	75.26	Very low	Yes	Yes	Yes	Stationary
PS-4	1984–2020	3.74	8.25	Yes	No	No	Ephemeral
PS-5	1984–2020	Very low		No	No	No	Stable
PS-6	1984–2020	Very low		No	No	No	Stable
PS-7	1984–2020	12.48	Very low	Yes	Yes	Yes	Stationary
PS-8	1984–2004	6.16	11.24	Yes	Yes	Yes	Stationary
	2005–2020		17.42				
PS-9	1984–2020	Very low		No	No	No	Stable
PS-10	1984–2020	Very low		No	No	No	Stable
PS-11	1984–2020	Very low		No	No	No	Stable
PS-12	1984–2020	63.65	Very low	Yes	No	No	Stationary
PS-13	1984–2020	31.98	6.44	Yes	No	No	Stationary
PS-14	1984–2020	Very low		Yes	No	No	Stable
PS-15	1984–2020	9.46	17.69	Yes	No	No	Stationary
PS-16	1984–2020	Very low		No	No	No	Stable
PS-17	1985–2019	2.68	Very low	No	Yes	No	Ephemeral
PS-18	1984–2003		17.90	Yes	Yes	Yes	Stationary
	1984–2020	3.29					
PS-19	1984–2020	10.46	15.13	Yes	No	No	Stationary
PS-20	1992–2006	156.93		Yes	Yes	Yes	Stationary
	2007–2012	−13.29					
	2013–2016	−135.30					
	1984–2020		1.92				
PS-21	1984–1991	51.99	21.69	Yes	Yes	Yes	Ephemeral
PS-22	1986–2006	55.72		Yes	Yes	Yes	Stationary
	2007–2014	−79.98	−17.70				
	2015–2020	42.06					
PS-23	1984–2020	Very low		No	No	No	Stable
PS-24	2003–2020	3.08	−9.27	No	Yes	Yes	Ephemeral
PS-25	1984–2012	35.49	3.58	Yes	Yes	Yes	Stationary
	2012–2020		6.91				
PS-26	1984–2020	1.13	1.67	Yes	Yes	Yes	Stationary
PS-27	1984–2020	134.92	−167.65	Yes	Yes	No	Ephemeral

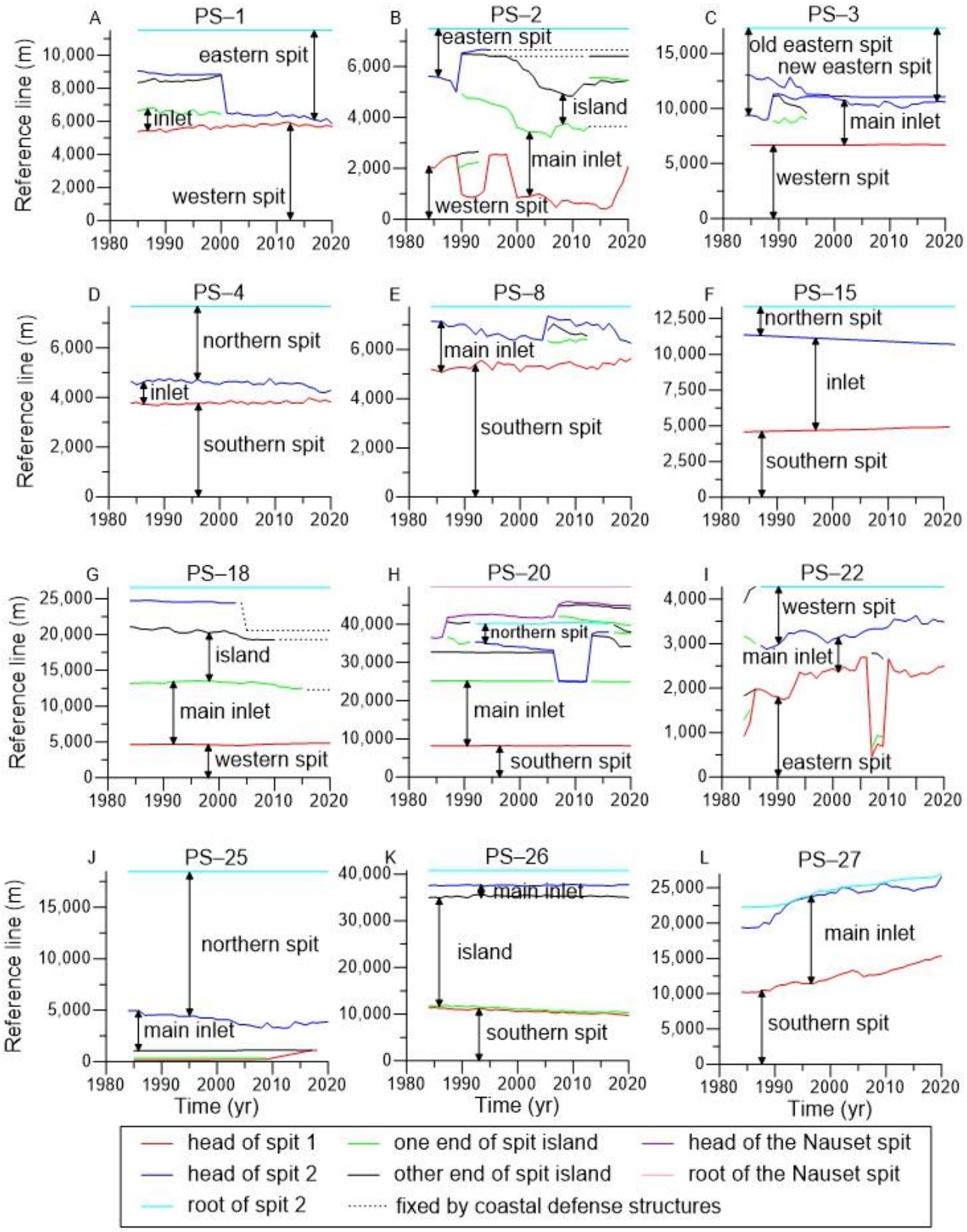

Figure 5. Geomorphological evolution (1984–2020) of some of the paired spits identified at the mouths of interdistributary bays of deltas (PS-1 to PS-3) and within channels (PS-4 to PS-27). Annual distances (m) for the head of the spits and ends of island are plotted on a reference line defined from the root of the two spits. (**A**) PS-1, (**B**) PS-2, (**C**) PS-3, (**D**) PS-4, (**E**) PS-8, (**F**) PS-15, (**G**) PS-18, (**H**) PS-20, (**I**) PS-22, (**J**) PS-25, (**K**) PS-26, (**L**) PS-27.

Three morphodynamic patterns for paired spits can be defined following the geomorphological evolution in the last decades of the twenty-seven systems analyzed (Table 2 and Figure 6). The first pattern corresponds to the stable systems, which are the eight systems of paired spits with very low progradation rates, and imperceptible geomorphological changes in the study period. Among them, PS-6 shows evidence of previous breaching and degradation of the central sector of the southern spit, but its progradation during the study period is very low. Another set of thirteen paired spits can be classified as stationary systems, with higher progradation rates and successive processes within a few decades of breaching or degradation of some spit, followed by the formation of new spits. PS-7 shows evidence of a previous degradation of the northern spit and the formation of the new spit in this margin of the channel is very slow. PS-6 can be considered an intermediate case between stable and stationary, as it shows evidence of previous breaching of the southern spit in its central sector, but the present progradation rate are very low.

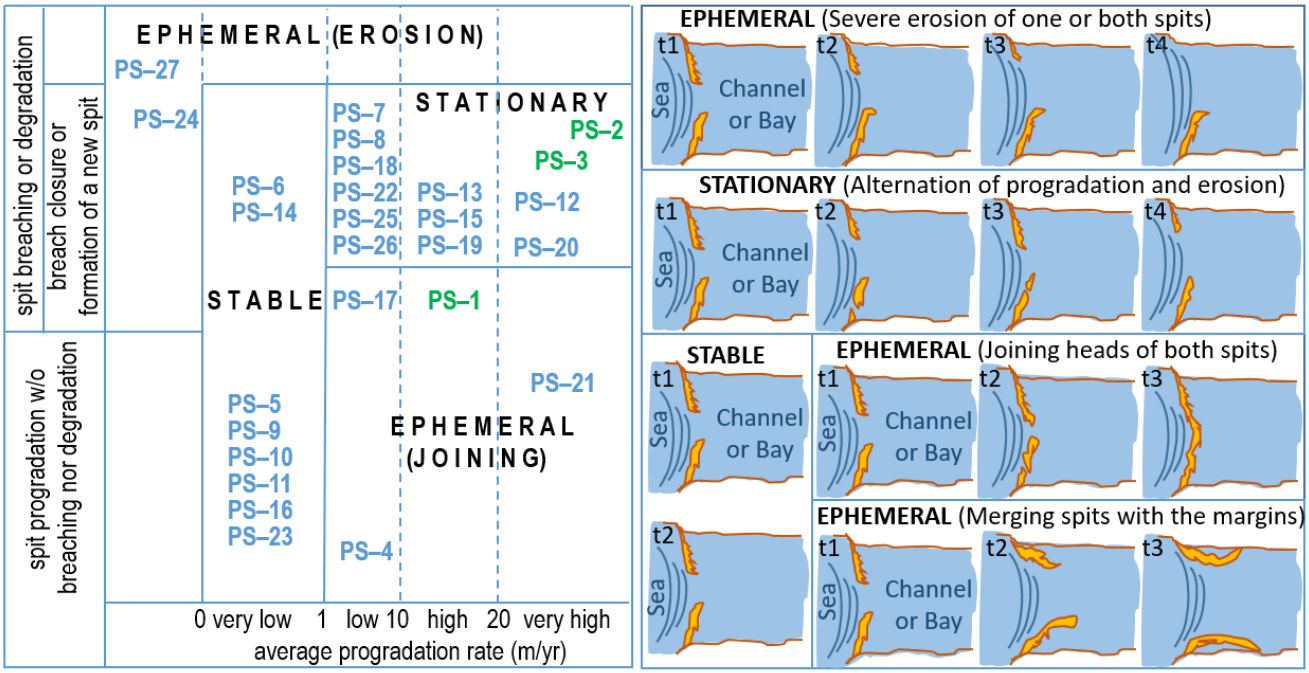

Figure 6. Morphodynamic patterns. Left: classification of stable, stationary, or ephemeral morphodynamic patterns of paired spits at the mouths of interdistributary bays of deltas (PS-1 to PS-3, green font) and within coastal channels (PS-4 to PS-27, blue font). Right: Synoptic description of the evolution for each morphodynamic pattern; the ephemeral (i.e., unstable) morphodynamic pattern includes three subtypes.

The third morphodynamic pattern corresponds to six unstable systems. They include PS-1 and PS-4, because the progradation of their heads will determine the near merging of the two spits and, consequently, these paired spits are ephemeral (Table 2, Figure 5A,D). Another type of unstable configuration occurs when the heads of the paired spits join to the respective sides of the channel. Thus, the two small spits observed in 1984 between Tuckernuck and Muskeget islands (PS-21) progressively rotated, erosion broke the western spit in 1991, and the heads of both spits merged their respective islands in 1994. Thus, the paired spits configuration of PS-21 disappeared. Similarly, the progradation of the two spits of PS-17 trended towards their respective margins, in the interior of the Strait of Canso. The progradation of the western spit towards the mainland of the Nova Scotia Peninsula was closing the lagoon entrance, decreasing its width to only about 4 m in 2019, while the head progradation of the eastern spit was towards the mainland of Cape Breton Island, with a lagoon entrance in 2020 of only 22 m in width (Figure 4P). The third type of unstable morphodynamic is due to high and continuous erosion, ultimately leading to the

permanent disappearance of one of the spits. The neck of the Tigres spit was breached in March 1962. Later, converging paired spits PS-27 developed on both sides of the inlet, and the southern spit tied to the mainland. However, the northern spit progressively eroded (negative progradation rate, Table 2) until it disappeared completely in 1993. Subsequently, since 2003, an incipient and very narrow spit started to develop, but disappeared again in 2019 due to severe erosion (Figure 5L). Therefore, the paired spits system has become ephemeral, while two other spits are developing northward in the mainland. Similarly, the length of the western spit of PS-24 within the Safaga Strait is decreasing; it virtually disappeared in 2011 and thereafter does not reach its previous size.

3.3. Hydrodynamics

The paired spits analyzed are located in a wide range of tide and wave regimes. Most of them (81.48%) are on microtidal coasts, except PS-9, PS-11, PS-12, PS-13 and PS-16, which are on mesotidal ones (Table 1). The wave regimes affecting the paired spits, considering their offshore wave pattern and shoreline orientation, includes unidirectional (51.85%), bidirectional (37.04%) and even multi-directional (11.11%) cases. The mean annual offshore Hs for the dominant component ranges between 0.45 and 1.84 m, and between 0.44 and 2.08 m for the second component. Peak periods include wind waves (53.84%), swell (28.21%) and intermediate (17.95%) waves (Table 3). Most of them are located on wave-dominated coasts, but there are also some others on mixed-energy or tide-dominated coasts.

PS-16, located in the sheltered Salish Sea, presents a mesotidal range (2.26 m) and offshore unidirectional wind waves with mean offshore Hs of 0.51 m from the SE; therefore, it can be classified as a tide-dominated environment. Progradation rates of the two spits are very low and the morphodynamic pattern is stable, without spit degradation or breaching. The remaining paired spits on mesotidal coasts (Table 1) are located in SW Alaska and are either tide-dominated (PS-9) or mixed-energy environments (PS-11, PS-12, PS-13). Offshore Hs are lower than 1.2 m for PS-9 and PS-11, which show a stable morphodynamic pattern. In contrast, the swell in PS-12 and PS-13, with a mean offshore Hs above 1.5 from the SSW (and above 2 m for the second component from the NW for PS-12), determine that the progradation rates are very high for the western spits of both systems, developed eastward from Tugidak Island, but low and very low for the eastern spits, developed westward from Sitkinak Island (Table 2 and Figure 4L).

Another important factor, along with waves and tides, is the formation of ice sheets in winter near the coast, as well as coastal snowfall and freezing, which were observed in satellite imagery and confirmed by gaps in ERAS5 wave data series for 51.85% of the paired spits analyzed in this study. This factor is most relevant for paired spits located in the Beaufort Sea (PS-1, PS-7 and PS-8) and the Kara Sea (PS-4 to PS-6), which are under wave attack for only 30–40% of the year, but was also identified for paired spits located in the Bering Sea (PS-10, PS-11 and PS-14), Gulf of Alaska (PS-9, PS-12 and PS-13), Gulf of St. Lawrence (PS-17) and the Sea of Okhotsk (PS-19), where exposure to wave influence is greater. The progradation rates of this set of paired spits range from very low to very high (Table 2, Figure 6), implying that they show stable (PS-5, PS-6, PS-9, PS-10, PS-11, PS-14), stationary (PS-7, PS-8, PS-12, PS-13, PS-19) and even ephemeral (PS-1, PS-4, PS-17) morphodynamic patterns. Wave and tide action in the period of the year free of ice sheets and coastal freeze-up determines the morphodynamic pattern.

Six other paired spits are located in sheltered seas with microtidal range and unidirectional or bidirectional wind waves of mean annual offshore Hs of 0.77 m or less (Table 3), as is the case of the paired spits found in the Adriatic Sea (PS-2, PS-3), Baltic Sea (PS-15), Black Sea (PS-18), Red Sea (PS-24) and Gulf of California (PS-21). Their progradation rates vary from low to very high and they are characterized by a stationary or ephemeral (erosional) morphodynamic pattern, with alternating erosion (degradation, breaching) and spit accretion (closure of inlets, formation of new spits), except in the Gulf of California where low energy waves explain that PS-21 shows low progradation rates, without significant morphological changes, and consequently a stable pattern (Table 2).

Table 3. Offshore wave (2018–2021): Percentage of the year free of ice-sheet formation; unidirectional, bidirectional, or multi-directional wave regime; frequency (%), mean annual and 95% percentile of Hs (m), approach direction and Tp (s) of the first and second component. The Tp includes wind waves (w), swell (sw) and intermediate (i) types.

Paired Spit	Wave Data Point		% Year	Wave Regime	1st Component					2nd Component				
	Latitude	Longitude			Freq	Hs	P95	Dir	Tp	Freq	Hs	P95	Dir	Tp
PS-1	69.71°N	141.3°W	33.21	Bi	21.71	0.85	2.12	ENE	w	11.34	0.80	1.77	NW	w
PS-2	44.75°N	12.28°E	100.00	Uni-	37.45	0.45	1.23	SE	w					
PS-3	44.79°N	12.47°E	100.00	Bi-	45.77	0.57	1.66	ENE	w	37.09	0.44	1.15	SE	w
PS-4	74.94°N	86.05°E	31.76	Bi-	9.27	0.74	1.67	NNE	w	9.04	0.79	1.98	NW	i
PS-5	73.09°N	69.50°E	40.93	Uni'-	18.71	1.03	2.47	WSW	w					
PS-6	70.16°N	125.31°W	31.07	Bi-	14.00	0.83	1.85	NW	w	10.01	0.72	1.56	ENE	
PS-7	69.69°N	125.37°W	31.07	Uni-	14.51	0.66	1.54	NNW	w					
PS-8	69.50°N	138.98°W	37.98	Uni-	17.72	0.53	1.07	ENE	w					
PS-9	59.45°N	153.50°W	100.00	Bi-	25.06	1.11	2.49	WNW	w	21.59	1.42	2.88	NE	w
PS-10	59.38°N	164.57°E	79.36	Uni-	29.20	1.64	3.75	E	sw					
PS-11	58.59°N	161.24°W	91.51	Bi-	40.41	1.06	2.35	SW	sw	15.76	1.31	2.69	ESE	w
PS-12	56.64°N	154.33°W	100	Bí-	57.22	1.55	3.13	SSW	sw	15.41	2.05	3.88	NW	i
PS-13	56.41°N	154.43°W	100	Uni-	57.68	1.77	3.57	SSW	sw					
PS-14	55.14°N	163.48°W	100	Uni-	65.79	1.42	3.10	W	sw					
PS-15	54.43°N	10.94°E	100	Bi-	34.47	0.68	1.54	WNW	w	18.07	0.76	1.61	SW	w
PS-16	48.52°N	123.28°W	100	Uni-	15.63	0.51	1.12	SE	w					
PS-17	45.74°N	61.53°W	96.44	Uni-	38.54	1.07	2.60	NNW	w					
PS-18	45.05°N	36.56°E	100	Bi-	40.11	0.77	1.79	NNE	w	36.73	0.68	2.60	SW	w
PS-19	43.69°N	145.32°E	92.13	Bi-	37.48	0.78	1.54	SE	sw	21.93	1.13	2.20	NNW	sw
PS-20	41.45°N	70.01°W	100	Multi-	26.91	0.89	1.86	SSE	i	18.95	1.35	2.99	ENE	sw
PS-21	41.32°N	70.27°W	100	Multi-	47.45	1.35	2.26	SSW	i	12.69	0.97	1.90	ESE	i
PS-22	41.25°N	70.26°W	100	Multi-	47.60	1.18	2.43	SSW	i	12.86	1.04	2.01	ESE	i
PS-23	28.80°N	112.16°W	100	Uni-	29.31	0.48	0.99	SSE	w					
PS-24	27.00°N	34.20°E	100	Uni-	100	0.68	1.31	NN	w					
PS-25	24.55°N	111.87°W	100	Uni-	44.06	1.19	1.60	SW	sw					
PS-26	24.30°N	111.66°W	100	Uni-	45.81	1.16	1.57	SW	sw					
PS-27	16.77°S	11.68°E	100.00	Uni-	100	1.84	2.80	SSW	sw					

The rest of the paired spits are located on microtidal open coasts of the Pacific and Atlantic oceans, under influence of swell or intermediate (6 to 9 s) waves with mean annual Hs varying from higher than 1.15 m to 2.8 m (Table 3), i.e., they are the paired spits under the most energetic waves, and consequently they are highly dynamic systems, with stationary or ephemeral morphodynamic patterns. The paired spits in Nantucket Sound (PS-20, PS-21, PS-22) are the only ones below an offshore multi-directional wave regime, but their different coastal orientation determines that PS-20 is mainly affected by ENE swell and SSE intermediate waves, while PS-21 and PS-22 are more influenced by SSW and ESE intermediate waves. Paired spits in Almejas Bay (PS-25, PS-26; Figure 4W) are below the influence of SW swell waves, with similar offshore Hs for both systems, but very high progradation rates for El Cisne spit, and low rates for the other three spits (Table 2). Finally, PS-27 lies under the strongest waves, with a unidirectional approach direction from the

SSW swell and annual offshore Hs of 2.8 m (Table 3), which determines the intense erosion of this ephemeral system (Figure 5L).

3.4. Anthropization of the Paired Spits

Most of the paired spits identified in this study are found in natural coasts, with no direct anthropogenic disturbance. In fact, some of them are nature reserves. Thus, for example, Demarcation Bay (PS-1), as well as Tugidak and Sitkinak islands, where are located PS-12 and PS-13, are Alaska National Wildlife Refuges, and for the PS-15, the Krummsteert spit and the outer half of the Graswarder–Heiligenhafen spit are two nature reserves. However, other paired spits analyzed in this study show the impact of local human activities (Table 4).

Table 4. Local human impacts and consequent classification of the paired spits at the mouth of interdistributary bays of deltas (PS-1 to PS-3) and within coastal channels (PS-4 to PS-27) from natural, to rural, semi-urban, urban, or artificial coasts.

Paired Spits	Longer Spit				Shorter Spit			
	Houses & Roads	Bridges	Seawalls	Type	Houses & Roads	Bridges	Seawalls	Type
PS-1	No	No	No	Natural	No	No	No	Natural
PS-2	No	No	Yes	Rural	No	No	Yes	Rural
PS-3	No	No	No	Rural	Yes	No	No	Semi-urban
PS-4	No	No	No	Natural	No	No	No	Natural
PS-5	No	No	No	Natural	No	No	No	Natural
PS-6	No	No	No	Natural	No	No	No	Natural
PS-7	No	No	No	Natural	No	No	No	Natural
PS-8	No	No	No	Natural	No	No	No	Natural
PS-9	No	No	No	Natural	No	No	No	Natural
PS-10	No	No	No	Natural	No	No	No	Natural
PS-11	No	No	No	Natural	No	No	No	Natural
PS-12	No	No	No	Natural	No	No	No	Natural
PS-13	No	No	No	Natural	No	No	No	Natural
PS-14	No	No	No	Natural	No	No	No	Natural
PS-15	Yes	No	Yes	Semi-urban	No	No	No	Natural
PS-16	Yes	No	No	Rural	Yes	No	Yes	Rural
PS-17	No	Yes	Yes	Rural	Yes	No	Yes	Semi-urban
PS-18	Yes	No	No	Urban	Yes	Yes	Yes	Urban
PS-19	Yes	No	Yes	Semi-urban	No	No	No	Natural
PS-20	No	No	No	Natural	No	No	No	Natural
PS-21	No	No	No	Natural	No	No	No	Natural
PS-22	Yes	No	No	Semi-urban	No	No	No	Natural
PS-23	No	No	No	Natural	No	No	No	Natural
PS-24	Yes	No	No	Natural	No	No	No	Natural
PS-25	No	No	No	Natural	Yes	No	No	Semi-urban
PS-26	No	No	No	Natural	No	No	No	Natural
PS-27	No	No	No	Natural	No	No	No	Natural

The Scardovari lagoon, in the Po delta, presented in 1985 natural paired spits (PS-2) at the mouth, with a stationary morphodynamic pattern including breaching of the eastern spit and formation of a baymouth barrier island. However, since 1995 several stone reefs have progressively fixed the shoreline of the two spits and the central island; the channel trough the eastern spit was also fixed to keep this lagoon open (Figure 5B).

The Goro lagoon (PS-3) is located to the west of the Scardovari lagoon. On the eastern side, a small bridge and some other minor structures were built in the head of the oldest spit, which remains stable after previous high erosion from 1989 to 1995, while a new spit developed seaward (Figure 5C). The western spit is occupied in the middle sector by buildings for tourist activity.

The Graswarder–Heiligenhafen spit (PS-15) shows high human occupation on the neck, including buildings, a marina on the inner side and coastal defense structures on the seaward side to prevent erosion. On the other side of the channel, human occupation of the Krummsteert spit (S of Fehmarn Island) is very low, with the only presence of a lighthouse, a few houses, and some agricultural land close to the beginning of the spit.

The James spit (PS-16), in the eastern margin of Cordova Channel, contains a road, a small marina in the inland, close to the head, while a stone seawall was constructed to avoid erosion of the neck. On the opposite side, Cordova spit shows no significant human occupation, but only a dirt road and isolated house.

In the Strait of Canso, the neck and some other areas near the head of the eastern spit of PS-17 are secured by boulders to prevent shore erosion. However, in 2007, a small breach opened in the middle of the spit. There is also a small bridge from the head of this eastern spit to the mainland of Cape Breton Island. The western spit, developed from the Ontario Peninsula, contains only a few buildings and a large electricity tower at the neck of the spit.

The western spit of PS-18, in the Kerch Strait, shows high human occupation with an axial road, buildings and tourism infrastructures by the seaside, as well as an industrial harbor in the inner part. In the northern sector of the Tuzla spit island, there was, from before 1984, a small harbor and a village that grew progressively, while the southern end of the island was attached by coastal defense structures since 2007. The Tuzla spit, on the eastern margin of the Kerch Strait, showed no local human alterations until 2003, when it was lengthened by artificial nourishment, the northern end was fixed by the construction of two stone-filled blocks in 2004, and construction of a motorway began on it. In 2015, the motorway and a railway linked the Tuzla spit to Tuzla Island by a bridge and another bridge linked the island to the eastern margin of the Kerch Peninsula. Therefore, both spits and the central spit island currently show high human disturbance.

At the southern end of the Nemuro Strait (also named Notsuke Strait or Kunashirsky Strait) is located PS-19. On the western margin, the Notsukezaki spit, from Hokkaido Island, is the largest sand spit in Japan, and shows strong human interventions, including an axial road, scattered buildings, several groins, and a seawall that is virtually continuous along its entire length, strongly fixing the shoreline except at the far end of the head. On the opposite side, two spits at the southern end of Kunashir Island (Kuril Archipelago) show no human disturbance, the smaller of which is also at the southern entrance to the Nemuro Strait.

The western spit of PS-24, in the Safaga Strait (Red Sea) developed from the head of a cuspate foreland with high human occupation related to the expansion of the urbanization of the city of Safaga in recent decades, prevents sediment input to the western margin of the strait. This cuspate foreland includes a small marina to the north, which is locally trapping sediments, and an industrial harbor to the south. On the root of the western spit, there is a house and a small marina. In contrast, the eastern spit of PS-24, on Safaga Island, is free of local human disturbance, except a dirt road.

At the northern entrance to Almejas Bay, near the head of the western spit of PS-25 there are remains of some abandoned buildings and a deserted small harbor. In contrast, the eastern spit of PS-25 and the two spits of PS-26 at the southern entrance to Almejas Bay are pristine coasts.

4. Discussion

4.1. Hydrodynamic Control

Wave-induced currents and associated littoral drift are the main factors controlling spit morphodynamics [7,65,66]; however, tidal currents can be decisive for megatidal coasts [16]. The paired spits identified in this study were more frequent on microtidal coasts but can also be found on mesotidal coasts (Table 1). This distribution is similar to that of paired spits at the mouths of bays, estuaries and deltas, which mainly correspond to microtidal coasts, while only a few studies refer to paired spits on the mesotidal coasts of England [62–72], Ireland [37,73] and Spain [74], on the macrotidal coasts of England [23,24,75] or the megatidal coasts of France [16,76]. Considering the relative energy of waves versus tides, it was deduced that the formation of paired spits mainly occurs on wave-dominated coasts, but also on tide-dominated (PS-9, PS-16) and mixed-energy (PS-11, PS-12, PS-13) coasts. This is probably because spits are like other coastal barriers, which develop best in microtidal environments with intermediate conditions between wave-dominated and river-dominated coasts [77].

The formation of paired spits has been previously described for unidirectional [25,37] and bidirectional [27,30,38] wave regimes. In this study, convergent longshore drift leading to progradation of the two spits was identified under uni-, bi- and multidirectional offshore wave regimes (Table 3). In the case of deltas, the intense refraction due to their prominent morphology may explain that offshore bidirectional wave regimes give rise to unidirectional wave regimes for paired spits in interdistributary bays, as in the case of the Goro lagoon (PS-3) in the Po delta [78]. In other interdistributary bays of deltas, such as Demarcation Bay, the offshore bidirectional wave regime [79] explains the convergent progradation of the paired spits (PS-1).

The development of spits in the mouths of deltas is typical of wave-dominated deltas, and these spits tend to evolve rapidly [80], as is also the case of the paired spits analyzed in the interdistributary bays of deltas (PS-1, PS-2, and PS-3). Fluvial discharge is primarily responsible for sediment supply and the formation of successive delta lobes and interdistributary bays [81,82]. The natural tendency for sedimentary filling of the interdistributary bay by fine-grained organic-rich and clastic sediments [83–85], together with the high convergent progradation of the paired spits in the mouths of interdistributary bays (Table 2), suggest that these systems are rare because they are ephemeral under natural conditions (PS-1) and the inlet only remains open in the deltas because of high human intervention (PS-2 and PS-3). In fact, the breaching of the eastern spit of PS-1 was observed ot the beginning of the study period, as well as plotted in the nautical chart, but this minor inlet closed in 2000 and the convergent progradation continued (Figure 5A). The final closure or not of this interdistributary bay will be determined by the hydraulic blockage between the two spits due to tidal currents or minor Clarence River outfalls that flow directly into the interdistributary bay.

Accumulative features, such as spits and barriers, are common along many Arctic coasts [86], which explains why some of the paired spits identified in this study are also found on the Arctic coast (Figure 1 and Table 1). The development of ice shelves limits the effects of winds, waves, tides, and river outflows for nine months of an average year on Arctic coasts, i.e., except for the open-water season, typically from July to September [87,88], and similarly for other high-latitude regions. Analysis of monthly LANDSAT images and offshore-wave data series (Table 3) has shown that ice-sheet development and coastal freezing impede or delay the morphodynamic evolution of the paired spits in the Arctic Ocean, the Bering Sea, the Gulf of Alaska, the Kamchatka Peninsula, the Gulf of St. Lawrence, and the Sea of Okhotsk (PS-1, PS-4 to PS-11, PS-14, PS-17 and PS-19). This is a new factor not previously considered in the scientific literature on the hydrodynamic agents controlling the morphodynamics of paired spits.

The hydraulic blockages that allow the entrance between the convergent paired spits within channels to remain open, and even the degradation and development of new spits on behalf of their connection into a single barrier, is due to tidal currents flowing through

the channels [45,89]. The increase in local depth observed on the nautical charts of some study sites (Table 1), just between the two spits, is evidence of these strong currents through the channels. Most of the paired spits located at the entrance to the channels are oriented inwards of the channel, indicating the incoming dominance of the longshore drift, with the only exception being the Nemuro Strait (S Sea of Okhotsk), where the paired spits PS-19 are oriented outwards, i.e., related to the outgoing currents of the channel. In the Safaga Strait (Figure 4V), the paired spits SP-20 developed in the middle of the channel; the morphology, orientation and morphodynamics of these paired spits show that they are clearly related to a southward current flowing through the channel [90].

With regard to long-term evolution, sea-level oscillations will determine the evolution of these paired spits. The Holocene transgression favored the occurrence of offshore islands and, consequently, the development within the channels of tombolos [91] and paired spits. Similarly, on the Arctic coast, the Holocene transgression induced the formation of coastal bays, due to breaching of thermokarst lakes, and consequently favored the subsequent formation of barrier islands and spits [92], including paired spits. However, the present sea-level rise due to the impact of the anthropogenic climate change is a clear hazard for the future evolution of Arctic coasts [93] and the Po River delta [94], which include erosion risks for the paired spits developed at their interdistributary bays, as well as for the spits and paired spits developed within coastal channels [95].

4.2. Sediment Availability and Sedimentary Interactions

Good sediment availability is also necessary for the development of spits [29,87,96] and paired spits [97]. The dimensions of the spits (Figure 4 and Table 1), the intensity of shoreline progradation and the ability to develop new spits or regenerate old ones after degradation or breaching (Figure 5 and Table 2) are evidence of this sediment availability. Dimensions are similar in the mouths of the interdistributary bays of deltas, but usually very different at the entrance and within the channels, which indicate the different intensities of the longshore drift and sediment inputs in the latter.

In the interdistributary bays of deltas, the fluvial source of sediments for the paired spits can be from different rivers (PS-1, PS-3) or from the same river (PS-2). In fact, the sediment source for the development of the two spits of the Scardovari lagoon (PS-2), as well as the Scanno of Goro spit, in the eastern flank of the Goro lagoon (PS-3) are related to the modern Po River delta [40,42,98]. Progradation rates are similar for these three spits (Table 2), which is consistent with a similar fluvial discharge supply for the southern mouths of the delta [99,100]. The two paired spits constraining the Goro lagoon show similar lengths (Table 1, Figures 4C and 5C, but the sediment input for the Scanno of Volano spit, on the western flank, is lower and mainly due to littoral drift from the south [42,78], which is consistent with its very low progradation rate (Table 2).

In the medium-term temporal scale, another factor determining the evolution of deltas is subsidence, which allows for the erosion of the abandoned delta lobes, including their distal spits and islands [101]. The Scardovari and Goro lagoons are not related to the abandoned lobes of Po River delta, quite the contrary; however, these lobes have shown the highest subsidence rates of the entire Po River delta from 1967 to 2017. The zone of highest subsidence in the delta has been shifting from north to south since at least 1957 [102], implying an erosion risk for PS-2 and PS-3.

In coastal channels with good sediment availability, the development of cuspate forelands and tombolos in the wave-shadow central sector is common [103–106], whereas sediment scarcity favors the formation of long, narrow, and deep coastal channels [107], even though the channel morphology predicts the presence of cuspate forelands or tombolos [105,106,108]. Tombolos and cuspate forelands have developed as a result of sediment inputs from both channel entrances [4,25,104]. Paired spits within channels are also cuspate bedforms but are related to convergent longshore drift and sediment input toward a single channel entrance. Sediment supply for progradation of paired spits constraining channels can be due to cliff erosion upstream, as in the case of the Graswarder–Heiligenhafen

spit [109,110] of PS-15, at the western entrance to the Fehmarn Sound (Baltic Sea), or to littoral drift from spits, beaches, and dunes upstream [45,111]. Nevertheless, many times, sediment supply for spit progradation is also due to cannibalization of its own neck [112–114] as can be observed in the western spit of PS-12, or material scoured from the inlet can be the dominant source for spit accretion, as shown by [115] for the northern spit of PS-20.

Paired spits within coastal channels are, in general, of different lengths (Table 1). The high sediment availability in the Magdalena coastal plain (W coast of the Baja California Peninsula) is related to the development of large Pleistocene coastal dune sheets [116] and large Holocene spits constrain both entrances to Almejas Bay, i.e., the El Cisne spit (PS-25) at the northern entrance, as well as the Flor de Malva spit and the Creciente spit island (PS-26) at the southern entrance [117]. The dimensions and average progradation rates (1984–2020) of the El Cisne spit are higher than those for Creciente Island (Table 2), indicating a greater littoral drift at the northern spit. On the other hand, the small inlet between Creciente Island and the Flor de Malva spit is not closing and it shows a migration rate of 44.50 m/yr (1984–2020) to the southeast. This implies that the dominant longshore drift at the root of the spit is also to the southeast, i.e., similar to the direction of the inlet migration [2,118,119], because updrift migration of inlets only occurs for shorter periods, lasting months or years [115,120]. Therefore, this suggests the current existence of a divergent littoral drift from the middle of the Flor de Malva spit, as the progradation of the head of the Creciente spit island is westward (Figure 5K and Table 2). On the opposite channel margin, the western spits of PS-25 and PS-26, linked to Santa Margarita Island, are very short (Table 1), likely due to low sediment availability from the island, and progradation rates are also low (Table 2).

Spit migration has been described for single spits [19,22] and paired spits [121,122]. In this study, obtained by analysis of satellite images from 1984 to 2022, spit migration was identified in some paired spits systems (PS-7, PS-20, PS-22, PS-24, PS-25), but may also have occurred in others before the start of the study period. Therefore, spit migration is a possible process for sediment input and the development of paired spits at the entrance to channels or within them, due to the breaching of nearby spits and their migration along the shore towards the channel.

In any case, the source area of sediments for paired spit bounding interdistributary bays of deltas or channels is usually different for each spit, i.e., sediment supply is due to longshore drift from different coastal fringes for each margin of the bay or channel. However, sedimentary interactions between them can be expected when they are located on shallow coasts, the channel width is low and the development of the paired spits implies a significant decrease on the width of the interdistributary bay (PS-1) or channel (PS-4) (Table 1, Figure 4A,D,I), favoring sediment bypass through the inlet by several possible mechanisms [27]. On the other hand, the increase in depth in some of the inlets between the two paired spits is evidence of local intensification of the hydrodynamics due to constriction of the channel entrance (PS-11, PS-12, PS-13, PS-23). These currents and increased depth prevent the two spits from merging, but may generate increased head progradation rates, and consequently cannibalization of the neck of the spits.

Sedimentary interactions due to channel constriction can also be identified between nearby paired spits systems, such as PS-20, PS-21 and PS-22, located in different entrances of Nantucket Sound (NW Atlantic Ocean). The largest entrance to Nantucket Sound is located to the east, between Cape Cod and Nantucket Island. Outer Cape Cod is composed of two divergent spits, the Provincetown spit northward and the Nauset spit southward, due to Holocene reworking of glacial outcrop sediments by divergent longshore drift [123]. A historic inlet near the northern end of the Nauset spit is migrating downward, i.e., southward, even though it has temporarily migrated updrift developing paired spits [115,124]. The nodal point for the divergence of the longshore drift between the Provincetown and Nauset spits is also migrating southward [125,126], and, consequently, sediment input to the Nauset spit decreased. An extratropical storm in 1987 allows formation of a new inlet in

the Nauset spit off Chatham Light [127–129] and a spit island that subsequently migrated and elongated southward. In 1992, the northern end of the island elongated updrift and connected to the mainland, becoming a new spit (the northern spit of Figure 5H). In 2007, the southern end of this new spit merged with Monomoy Island [130], located at the northern margin of the main entrance to Nantucket Sound. Thus, this new spit together with the northern spit (named Great Point) of Nantucket Island are paired spits (PS-20), which bound the main entrance to Nantucket Sound (Figure 4S).

The northern spit of PS-20 breached in 2013 to become an island and was subsequently completely degraded by wave erosion (Figure 5H). Nevertheless, since 2007, a new inlet and spit island developed again by breaching of the Nauset spit off Minister's Point (Figure 5H); therefore, this island will probably join the mainland and/or Monomoy Island in the coming decades. A graphical reconstruction of the 1984–2020 morphodynamic evolution of the Nauset spit, the new spit southward, and Monomoy Island was reported by the NASA [131]. The reconstruction of the coastal evolution since 1846 has shown that this process of extension of the Nauset Spit to connect to Monomoy Island and the subsequent break-up is cyclical, repeats approximately every 150 years, and therefore, Monomoy Island is related to former spits and spit islands formed from the breaching of the Nauset spit [111,132]. The southward progradation rate of Monomoy Island is much lower than that for the southern spit developed from the breaching of the Nauset spit (Table 2), with values of 7.64 (1984–2006), 13.29 (2007–2012), and 6.36 m/yr (2013–2021). In 1971, a decrease of southward progradation of Monomoy Island was predicted, due to encroachment of the southern end of the island into two deep basins to the northeast and southeast [133]. However, this was not identified in the study period, and the increase of the progradation rate between 2007 and 2012, when Monomoy Island merged with the new spit developed from breaching of the Nauset spit, is remarkable. Perhaps, the decrease in southward progradation will occur in the near future.

On the southern margin of Nantucket Sound, two other paired spits (PS-21 and PS-22) were identified in Muskeget Channel, westward of Nantucket Island (Figure 4T), with recurved spits and the development of flood- and ebb-tidal deltas, denoting that they are controlled by both wave and tidal currents. The maximum narrowing of the main entrance to Nantucket Sound occurred from 2007 to 2012 (Figure 5H), when the new spit joined Monomoy Island (PS-20). This basically corresponds to the period when the head of the two spits of PS-22 eroded (2007–2014) and even developed a small inlet (2007–2009) from the breach of the eastern spit (Figure 5I). Water circulation on Nantucket Sound is tidally dominated [89]. Therefore, narrowing of the main entrance by the development of PS-20 generated the intensification of tidal currents through Muskeget Channel, where PS-21 and PS-22 are located. Subsequently, when the northern spit of PS-20 became an island again and was progressively eroded away (Figure 5H), widening the inlet between Monomoy Island and the Cape Cod mainland, the hydrodynamic outflow through the Muskeget Channel decreased and the paired spits of PS-22 again showed convergent progradation (Figure 5I). Contrary to the erosion of PS-22, the eastern spit of PS-21 developed a new ridge from 2007 to 2012, due to sediment input from the degradation of PS-22, but later eroded drastically when PS-22 progressively regained its convergent progradation. The western spit of PS-21 only developed in the first decades of the study period, but in the 1990s it migrated, rotated, and merged with its island, which has shown severe erosion and remodeling throughout the study period. Therefore, the combined analysis of PS-20, PS-21 and PS-20 shows that hydrodynamic and sedimentary interactions occur not only between the two paired spits of the same system, but even with other closer paired spits in the same channel. This provides evidence that they are not independent spits, but a complex system including several paired spits.

In contrast, in the case of channels with deep and very wide inlets between the paired spits, there is no evidence of sedimentary interactions between the two paired spits, such as PS-19 in the Nemuro Strait, where they are far apart and bathymetry only shows an intensification of currents very close to the western spit. Similarly, sedimentary interactions

are not clear between the two spits of PS-15, at the entrance to Fehmarn Sound. The Graswarder–Heiligenhafen spit, located in the north of the Peninsula of Wagria, has grown eastward by longshore transport for about 3000 years, with the addition of successive hooked ridges developed in intervals of about 150 years [134,135]. It shows a current progradation rate of 9.46 m/yr (1984–2022, Table 2), which is significantly higher than previous rates of 3.5 m/yr (1950–1985) after [109] or 2–3 m/yr suggested by [110]. In the same PS-15, the Krummsteert spit (S of Fehmarn Island) shows an even higher progradation rate (Table 2). However, both spits developed almost parallel to the channel margins, so that a merging of the two spits in the near future, or any other sedimentary interaction, is unlikely. All the same, the development of both spits implies a decrease to 75% of the original width at the mouth of the Fehmarn Sound, and consequently an intensification of the currents through it.

4.3. Morphogenetic Models and Morphodynamic Patterns of Paired Spits

Five conceptual models for the formation of paired spits were previously described at the mouth of bays and rivers (Figure 7): (i) the break of a coastal barrier, not necessarily a spit, by new fluvial outlets [68,74], hurricanes [23] or tsunamis [136,137]; (ii) convergent longshore drift in a narrow bay [25]; (iii) bidirectional longshore drift with hydraulic blockage by tidal currents or river flow in a bay or river mouth [26,120]; (iv) cutting of an estuarine detached spit by high-energy events [27–30]; and (v) convergence of two estuarine mouths and the associated spits [30]. In addition, previous studies in the Po River delta have already defined the presence of two spits in the mouths of both the Goro and the Scardovari lagoons [40–44], although none of these studies consider them as paired spits or relate their development to other baymouth spits. The presence of paired spits within channels has been succinctly reported [45–47]. Therefore, in this study, two new environments and conceptual models for the formation of convergent paired spits were described in detail and monitored, at the mouths of the interdistributary bays between two delta lobes of the same or different rivers (Figure 7F), and at the two margins of a channel, in the entrance or within it, usually for incoming, or exceptionally for outgoing, longshore drift (Figure 7G).

The development of paired spits in the interdistributary bays of deltas and within coastal channels was described for uni-, bi- and multidirectional wave regimes (Table 3). Therefore, they are under similar hydrodynamic patterns to conceptual models ii and iii but are located in different coastal environments. In fact, conceptual models i, iv, and v have only been reported in a few places [23,27–30,68,74,136,137]; therefore, they can be considered as unusual.

In addition to the new morphogenetic models for paired spits (Figure 7F,G), three morphodynamic patterns (stable, stationary and ephemeral) were defined for the subsequent geomorphological evolution of paired spits (Figure 6, Table 2). For stationary systems, the degradation and development of new spits is the key that allows them to maintain the paired spit configuration, i.e., to achieve a stationary equilibrium, oscillating between eroded to accretionary states, which resembles seasonal beach morphodynamics [138]. A stationary pattern was described for single spits, due to high erosion after breaching and subsequent closure of the inlet e.g., [14,139] or even total and fast degradation by tsunamis followed by the formation of a new spit [140]. Similarly, the eastern spit of PS-3 has undergone intense morphodynamics changes, including phases of rapid longshore growth, hooked ridges development, cannibalization, overwash, and breaching [98]. There are also intermediate cases between stable and stationary systems. For instance, a historical analysis of nautical charts shows a minor inlet developed in PS-14 from 1949 until before 1974 [47], but can currently be considered stable because average migration rates in recent decades (1984–2020) are very low (Figure 6). Some other paired spits show an unstable or ephemeral morphodynamic pattern. The filling of the interdistributary bay on the backshore of PS-1 and the disappearance of this coastal configuration with paired spits should be expected

on a medium-term scale, similar to the closure in previous centuries of the Sinoe lagoon, an interdis tributary bay in the southwest of the Danube delta [141,142].

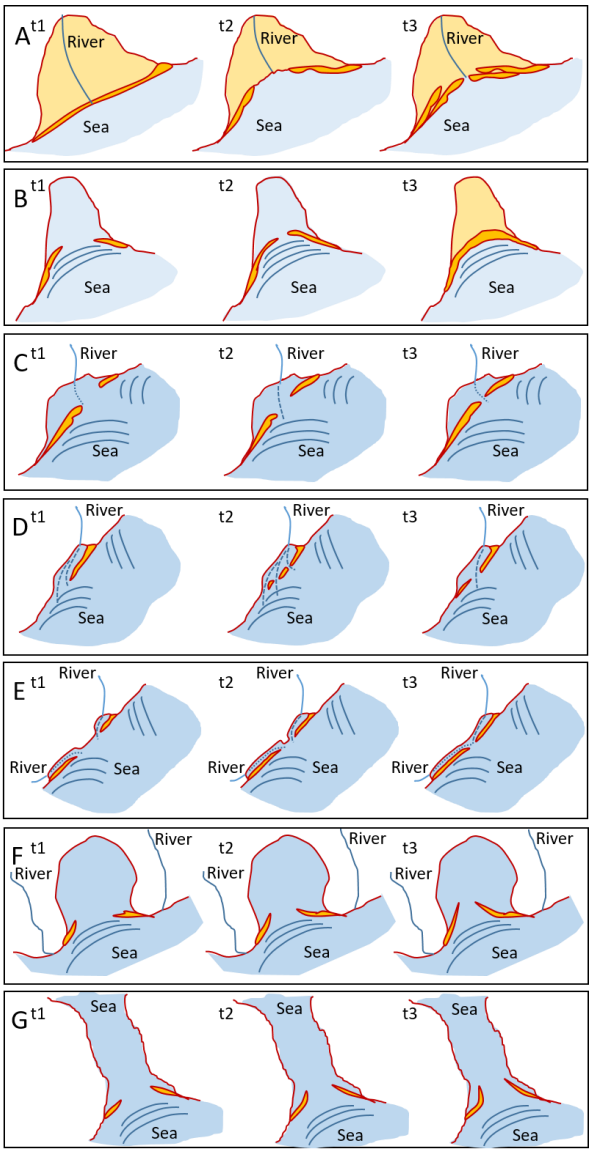

Figure 7. Conceptual models for formation of paired spits: (**A**) coastal barrier break; (**B**) convergent longshore drift in a narrow bay; (**C**) bidirectional longshore drift with hydraulic blockage; (**D**) cutting of a estuarine detached spit by high energy events; (**E**) convergence of two estuarine mouths and the associated spits; (**F**) convergent progradation from two delta lobes to the interdistributary bay (PS-1 to PS-3); and (**G**) convergent longshore drift from both margins to a channel entrance (PS-4 to PS-27) (Modified from [36]).

The three morphodynamic patterns adescribed above can also be applied to characterize the morphodynamics of paired spits at the mouths of bays and rivers. Most of them correspond to systems with a stable geomorphological configuration, while only a few studies have referred to spit breaching or degradation and the development of new spits [29,30,74,122,143]. The paired spits at the mouth of the Guadalquivir estuary (SW Spain), showed an initial stationary pattern, with degradation and the new formation of the southern spit (6900 to 2300 BP); subsequent intense progradation of the northern spit (2300 to 1000 BP) evolved to a stable pattern, where currently the southern spit is fixed by the sedimentary fill of the estuary mouth [74]. Another interesting case is that of the paired spit PS-17, in the Strait of Canso, because in the late 19th century there was an inlet

in the middle of the western spit (Church, 1878; in [144]), but nowadays this inlet does not exist, and the head of the spit is very close to the western margin of the channel. Therefore, it evolved from a stationary to an ephemeral pattern. Some other studies have described paired spits at river mouths that later disappeared, i.e., were ephemeral [28–30,145]. In summary, it can be deduced that paired spits can evolve from stationary to ephemeral or stable morphodynamic patterns and can even become relict bedforms from a stable pattern.

4.4. Anthropization of the Paired Spits

Most of the paired spits identified at the mouths of interdistributary bays of deltas and within channels have shown processes of degradation and the development of new spits; some other paired spits tended to develop a continuous sand barrier, or even to disappear (Table 2, Figure 6). Their intense sedimentary dynamics and geomorphological evolution, together with the remote location of many of them, explain why they have not been described before, whereas paired spits at the mouth of bays, estuaries and deltas have been described more extensively for the anthropized coast of England [23,24,67–72,75,146,147], Ireland [73,148,149], France [16,76], Spain [74], Russia [25], India [26,34,38], China [121,122], United States of America [29], Egypt [143], Senegal [150], Colombia [151], Brazil [30,39,152], and New Zealand [28,145]. Nevertheless, paired spits have also been described in natural coasts, at the mouths of bays in the Kamchatka Peninsula [25], and at the mouth of the Volta River delta, although the latter is heavily affected by the Akosombo dam [150,153].

The morphodynamics of many single spits are affected by natural climatic oscillations, such as ENSO [36,154–156] and NAO [76,157], as well as by human disturbances, ranging from global climate change, including sea-level rise and ice melting between other effects [158–161], to local impacts. Coastal defense structures have been built in many spits to avoid erosion, usually on the seashore [10], and more rarely on the bayside [162]. At other times, the artificial opening of channels for fishermen's navigation [163] or to prevent flooding [17] has generated severe erosion of the spits.

Similarly, paired spits at the mouths of bays, estuaries and deltas are often affected by local human activities, such as urbanization, dam construction, coastal defense structures, and dredging to keep channels open for navigation [143,147,149,150,153,164,165]. Elsewhere, degradation of baymouth spits by harbor development or other human disturbances is even more severe [122]. In contrast, most of the paired spits identified in this study are found on natural coasts (Table 4), with no direct anthropogenic disturbance. Therefore, they are ideal locations for environmental conservation plans. They are also very interesting places for the analysis of the impact of both natural climatic oscillations such as ENSO [30,121] and climate change, since in these paired spits ice melting, coastal erosion and flooding due to sea-level rise are not affected by interactions with other regional or local anthropogenic factors that may mask the impact of natural climatic oscillations and global climate change.

Other paired spits analyzed in this study show local human disturbances of very different intensities (Table 4). The paired spits with a higher human influence on their morphodynamics are PS-2 and PS-3, the two interdistributary bays located in the SW of the Po River delta. In fact, the historical and current evolution of the delta is strongly conditioned by human activities [40,166]. The modern delta was induced 400 years ago by the excavation of an artificial channel [167]. In the southern part of the delta, the development of the paired spits at the mouth of the Scardovari lagoon (PS-2) is relatively recent. The lagoon developed in the early 19th century, without paired spits at the mouth, and acquired its present shape in 1955 [168]. Later, the construction of reef stones after 1985 not only protected the coast from erosion, but even generated high sedimentation [169], keeping the lagoon open by artificial inlets. The Goro lagoon has progressively migrated southwards since the 16th century. The nautical charts show the presence of paired spits on the mouth of the Goro lagoon since the late 19th century [41]. The human impact on these paired spits (PS-3) is lower than those for the Scardovari lagoon (PS-2), despite the mouth

of the outlets has been also fixed by stone reefs. However, the bathymetry near the main entrance to the lagoon is very shallow [99] and dredging has been suggested [55].

The fixation of the spits by coastal defense structures, roads, railways, and big bridges are strong human disturbances on the geomorphology of the paired spits. Coastal defense structures are usually located on the neck of the spits (southern spit of PS-15, eastern spit of PS-16, both spits of PS-17) but sometimes they are almost along the whole seaside of the spits, as is the case with the Tuzla spit (PS-18) in the eastern margin of the Kerch Strait [170] and the Notsukezaki spit (PS-19) in the western margin of Nemuro Strait [171,172]. Fixing of the shoreline avoids breaching and the formation of spit islands. While head progradation of the spits can continue (PS-19), it can be drastically reduced due to the lack of sediment inputs from the neck (PS-18), or it can even increase, as indicated above for PS-2 [169]. Therefore, some paired spits with natural stationary morphodynamic patterns have evolved into a human-induced stable morphodynamic pattern (PS-18) or a human-induced ephemeral pattern by joining each spit with its margin of the channel (PS-17). Tuzla Island was formed due to breaching of the Tuzla spit (PS-18) in 1925 [173], which is characteristic of a stationary pattern. However, the shoreline of both Tuzla Island and the Tuzla spit has been progressively fixed since 2004 (Figure 5G) [170]. In other cases, there are only small villages or a few houses, which implies a change from natural to rural or semi-urban coast, but these human activities do not affect the natural morphodynamic pattern (eastern spit of PS-22, western spit of PS-25).

In an exceptional case, the coastal region has changed from high human occupation to a natural or nearly natural environment. Tigres Island was initially a 40-km long spit, with a well-established fishing village to the northeast. However, when the neck of the spit broke in 1962 and became an island, the village was abandoned [45], and currently is only visited by tourist excursions. The ephemeral (erosive) morphodynamic pattern of PS-27 has not been influenced by the previous urban development or any other human activity.

Coastal management, including implementation of coastal conservation areas and coastal defense structures, are usually only focused on one spit of the paired spits systems [147,165,174]. However, analysis of the hydrodynamics and sedimentary interactions, and models of the formation and morphodynamic patterns show that, rather than independent spits, the paired spits constitute a system, which should be taken into account for future coastal management plans. Mitigation measures, such as the construction of sand barriers and sediment replenishment, can help protect these vulnerable areas [14]. Nevertheless, at present, certain management approaches involve the removal of hard coastal defense structures that were previously used [162,175]

Spits are important coastal formations that protect coastal areas. However, the dynamics of these formations are extremely complex and can be influenced by multiple factors. To understand this complexity, it is essential for researchers and coastal managers to be aware of the different behaviors of spits. This may include analyzing their geometry, studying sedimentation and erosion on their surfaces, and identifying sediment transport processes, among other aspects. By emphasizing the complexities of these behaviors, these professionals can be equipped with the necessary tools to properly manage these coastal barriers. This will enable them to better decide how best to protect coastal areas and the communities living in them.

In the future, high-resolution monitoring will be integrated with operational wave models to create accurate systems for predicting coastal evolution at various temporal and spatial scales. In addition, combining advances in satellite monitoring with machine learning and data-assimilated modeling will help to resolve questions about the causes and effects of coastal erosion at large scales [176].

5. Conclusions

This study presented the first analysis of the global distribution and geomorphological description of paired spits developed both at the mouths of interdistributary bays of deltas (three systems) and within channels (24 systems). Two new environments and

conceptual models for the formation of paired spits were presented, in addition to the five morphogenetic models described in previous studies. The identified paired spits were mainly located at high or mid latitudes, and on microtidal coasts, although they have also been found at low latitudes and on mesotidal coasts. Longshore drift and wave erosion are the main control factors in their formation and development. Paired spits can be generated under multidirectional to unidirectional approach waves. The hydraulic blockage necessary for the development of these paired spits is mainly due to tide-induced currents, as well as minor fluvial outlets in the interdistributary bays. However, the formation of ice sheets at high latitudes prevents wave action and, therefore, delays the morphodynamic evolution of paired spits. The sediment source for the paired spits at the mouths of the interdistributary bays can be from the same river or from different rivers. The sediment source for the spit at each channel margin is from different coastal strips. Nevertheless, sedimentary interactions between the two paired spits can be identified, particularly when they are located on shallow coasts and when the heads of the spits are close together. These hydrodynamic and sedimentary interactions make clear that paired spits are a system, rather than independent spits. Hydrodynamic and sedimentary interactions were also identified between systems of paired spits located at different entrances of the same channel, which therefore constitute a complex system of paired spits.

The main morphodynamic processes that characterized the evolution of the paired spit analyzed were: convergent progradation from the head and/or from the middle of the spits, developing new hooked ridges; possible migration of the spits to the entrance or within the channel, as well possible rotation of the spits and even joining of the spits to their margin of the channel; spit erosion by degradation of the spits or the formation of breaches on the spits, where subsequently the spit islands can be degraded or the breach closed. As a result of convergent progradation, the width of the inlet between the heads of the two spits usually decreases, but sometimes it only migrates and sometimes it even increases. Three morphodynamic patterns were defined as a function of these processes: (i) a stable pattern, which corresponds to systems with average progradation rates below 1 m/yr, generally without breaching or the degradation of any of the spits; (ii) a stationary pattern, for systems with higher average progradation rates and alternating degradation or breaching of one of the spits with formation of new spits or closure of the breaches; and (iii) an unstable or ephemeral pattern, which includes three subtypes, the first due to severe erosion of one or both spits, the second due to the joining of the head of the two spits forming a single barrier, and the third when each spit merges with its channel margin. These three morphodynamic patterns can also be applied to paired spits in the mouths of bays or rivers. Furthermore, the morphodynamic pattern identified for each paired spits system in the decadal scale analysis may evolve in the medium and long term, as evidence historical charts and stratigraphic studies indicates.

Most of the paired spits are located on natural coasts. The geological uniqueness, wide geographical distribution, good ecologic conservation, and low human occupation of many of the paired spits analyzed allow them to be defined as sites of high scientific interest which are suitable as field laboratories for the analysis of the effect of natural climatic oscillations and climate change, as well as potential nature reserve areas. In other cases, anthropization of the spits ranges from agricultural and fishing activities to semi-urban and even urban development. Human actions also include the construction of coastal defense structures to avoid erosion in several of the spits.

Author Contributions: Conceptualization, J.A.-C.; Methodology, J.A.-C., Á.F.-B. and R.P.M.; validation, J.A.-C., A.C.R. and R.P.M.; formal analysis, J.A.-C., Á.F.-B., A.C.R. and L.P.; investigation, J.A.-C. and A.C.R.; resources, J.A.-C., Á.F.-B., R.P.M. and L.P.; data curation, J.A.-C. and A.C.R.; writing—original draft preparation, J.A.-C.; writing—review & editing, J.A.-C., Á.F.-B., R.P.M. and L.P.; visualization, J.A.-C.; supervision, J.A.-C. All authors have read and agreed to the published version of the manuscript.

Funding: This research received no external funding.

Data Availability Statement: The data presented in this study are available on request from the corresponding author.

Acknowledgments: We are grateful to reviewers who significantly contributed to the improvement of this paper. Wave data series have been supported by the European Centre for Medium-Range Weather Forecasts.

Conflicts of Interest: The authors declare no conflict of interest.

References

1. Bowman, G.; Harvey, N. Geomorphic evolution of a Holocene beach-ridge complex, LeFevre Peninsula, South Australia. *J. Coast. Res.* **1986**, *2*, 345–362.
2. Davis, R.A.; FitzGerald, D.M. *Beaches and Coasts*; Blackwell Publishing: Oxford, UK, 2004; 419p.
3. Shawler, J.L.; Hein, C.J.; Obara, C.A.; Robbins, M.G.; Huot, S.; Fenster, M.S. The effect of coastal landform development on decadal-to millennial-scale longshore sediment fluxes: Evidence from the Holocene evolution of the central mid-Atlantic coast, USA. *Quat. Sci. Rev.* **2021**, *7*, 107096. [CrossRef]
4. Evans, O.F. The origin of spits, bars and related structures. *J. Geol.* **1942**, *50*, 846–865. [CrossRef]
5. Otvos, E.G. Coastal barriers—Nomenclature, processes, and classification issues. *Geomorphology* **2012**, *139–140*, 39–52. [CrossRef]
6. Davis, R.A. Barrier Island Systems—A Geologic Overview. In *Geology of Holocene Barrier Island Systems*; Davis, R.A., Ed.; Springer: Berlin/Heidelberg, Germany, 1994; pp. 1–46. [CrossRef]
7. Ashton, A.D.; Nienhuis, J.; Ells, K. On a neck, on a spit: Controls on the shape of free spits. *Earth Surf. Dyn.* **2016**, *4*, 193–210. [CrossRef]
8. Cartera, R.W.G.; Orford, J.D.; Jennings, S.C. The recent transgressive evolution of a paraglacial estuary as a consequence of coastal barrier breakdown: Lower Chezzetcook Inlet, Nova Scotia, Canada. *J. Coast. Res.* **1990**, *9*, 564–590.
9. Kraus, N.C.; Patsch, K.; Munger, S. Barrier beach breaching from the lagoon side, with reference to Northern California. *Shore Beach* **2008**, *76*, 33–43.
10. Bastos, L.; Bio, A.; Pinho, J.L.S.; Granja, H.; da Silva, A.J. Dynamics of the Douro estuary sand spit before and after breakwater construction. *Estuar. Coast. Shelf Sci.* **2012**, *109*, 53–69. [CrossRef]
11. Behrens, D.K.; Bombardelli, F.A.; Largier, J.L.; Twohy, E. Episodic closure of the tidal inlet at the mouth of the Russian River—A small bar-built estuary in California. *Geomorphology* **2013**, *189*, 66–80. [CrossRef]
12. Kumar, A.; Narayana, A.C.; Jayappa, K.S. Shoreline changes and morphology of spits along southern Karnataka, west coast of India: A remote sensing and statistics-based approach. *Geomorphology* **2010**, *120*, 133–152. [CrossRef]
13. Green, A.; Cooper, J.A.G.; LeVieux, A. Unusual barrier/inlet behaviour associated with active coastal progradation and river-dominated estuaries. *J. Coast. Res.* **2013**, *69*, 35–45. [CrossRef]
14. Bateman, M.D.; McHale, K.; Bayntun, H.J.; Williams, N. Understanding historical coastal spit evolution: A case study from Spurn, East Yorkshire, UK. *Earth Surf. Process. Landf.* **2020**, *45*, 3670–3686. [CrossRef]
15. Hoang, V.C.; Tanaka, H.; Mitobe, Y. Estuarine morphology recovery after the 2011 Great East Japan earthquake tsunami. *Mar. Geol.* **2018**, *398*, 112–125. [CrossRef]
16. Robin, N.; Levoy, F.; Anthony, E.J.; Monfort, O. Sand spit dynamics in a large tidal-range environment: Insight from multiple LiDAR, UAV and hydrodynamic measurements on multiple spit hook development, breaching, reconstruction, and shoreline changes. *Earth Surf. Process. Landf.* **2020**, *45*, 2706–2726. [CrossRef]
17. Gunasinghe, G.P.; Ruhunage, L.; Ratnayake, N.P.; Ratnayake, A.S.; Samaradivakara, G.V.I.; Jayaratne, R. Influence of manmade effects on geomorphology, bathymetry and coastal dynamics in a monsoon-affected river outlet in Southwest coast of Sri Lanka. *Environ. Earth Sci.* **2021**, *80*, 238. [CrossRef]
18. Bhattacharya, J.P.; Giosan, L. Wave-influenced deltas: Geomorphological implications for facies reconstruction. *Sedimentology* **2003**, *50*, 187–210. [CrossRef]
19. Van Maren, D.S. Barrier formation on an actively prograding delta system: The Red River delta, Vietnam. *Mar. Geol.* **2005**, *224*, 123–143. [CrossRef]
20. Ashton, A.D.; Giosan, L. Wave-angle control of delta evolution. *Geophys. Res. Lett.* **2011**, *38*, L13405. [CrossRef]
21. Anthony, E.J. Wave influence in the construction, shaping and destruction of river deltas: A review. *Mar. Geol.* **2015**, *361*, 53–78. [CrossRef]
22. Dan, S.; Stive, M.J.; Walstra, D.J.R.; Panin, N. Wave climate, coastal sediment budget and shoreline changes for the Danube Delta. *Mar. Geol.* **2009**, *262*, 39–49. [CrossRef]
23. Ward, E.M. *English Coastal Evolution*; Methuen & Co. Ltd.: London, UK, 1922; 105p.
24. Lovegrove, C.H. Old shorelines near Camber Castle. *Geog. J.* **1953**, *119*, 200. [CrossRef]
25. Zenkovich, V.P. *Processes of Coastal Development*; Wiley-Interscience: New York, NY, USA, 1967; 751p.
26. Kunte, P.D.; Wagle, B. Spit evolution and shore drift direction along South Karnataka Coast, India. *G. Giol.* **1991**, *153*, 71–80.
27. FitzGerald, D.M.; Kraus, N.C.; Hands, E.B. *Natural Mechanisms of Sediment Bypassing at Tidal Inlets, Coastal and Hydraulics Engineering Technical Note IV–30*; United States Army Engineer Research and Development Center: Vicksburg, MS, USA, 2000; 10p.
28. Hume, T.M.; Herdendorf, C.E. Factors congtrolling tidal inlet characteristics on low drift coasts. *J. Coast. Res.* **1992**, *8*, 355–375.

29. Aubrey, D.G.; Gaines, A.G. Rapid formation and degradation of barrier spits in areas with low rates of littoral drift. *Mar. Geol.* **1982**, *49*, 257–277. [CrossRef]
30. Alcántara-Carrió, J.; Dinkel, T.M.; Portz, L.; Mahiques, M.M. Two new conceptual models for formation and degradation of baymouth spits by longshore drift and fluvial discharge (Iguape, SE Brazil). *Earth Surf. Process. Landf.* **2018**, *43*, 695–709. [CrossRef]
31. Zenkovitch, V.P. On the genesis of the cuspate spits along lagoon shores. *J. Geol.* **1959**, *67*, 269–277. [CrossRef]
32. Jensen, J.B.; Stecher, O. Paraglacial barrier-lagoon development in the late Pleistocene Baltic Ice Lake, southwestern Baltic. *Mar. Geol.* **1992**, *107*, 81–101. [CrossRef]
33. Boggs, D.A.; Boggs, G.S.; Eliot, I.; Knott, B. Regional patterns of salt lake morphology in the lower Yarra Yarra drainage system of Western Australia. *J. Arid Environ.* **2006**, *64*, 97–115. [CrossRef]
34. Mahanty, M.M.; Mohanty, P.K.; Pradhan, S.; Samal, R.N.; Ranga Rao, V. Spit and inlet morphodynamics of a tropical coastal lagoon. *Mar. Geod.* **2019**, *42*, 130–165. [CrossRef]
35. Rosen, P.S. Origin and processes of cuspate spit shorelines. In *Estuarine and Research. Vol II Geology and Engineering*; Academic Press: New York, NY, USA, 1975; pp. 77–92.
36. Alcántara-Carrió, J.; Caicedo, A.C.; Hernández, J.; Jaramillo-Velez, A.; Manzolli, R.P. Sediment bypassing from the new human-induced lobe to the ancient lobe of the Turbo delta (Gulf of Urabá; southern Caribbean Sea). *J. Coast. Res.* **2019**, *35*, 196–209.
37. O'Shea, M.; Murphy, J. Predicting and monitoring the evolution of a coastal barrier dune system postbreaching. *J. Coast. Res.* **2013**, *29*, 38–50. [CrossRef]
38. Avinash, K.; Deepika, B.; Jayappa, K.S. Evolution of spit morphology: A case study using a remote sensing and statistical based approach. *J. Coast. Conserv.* **2013**, *17*, 327–337. [CrossRef]
39. Alcántara-Carrió, J.; Mahiques, M.M.; Portz, L. Paired baymouth spits. In *Encyclopedia of Coastal Sciences*; Finkl, C.W., Makowski, C., Eds.; Springer International Publishing: Cham, Switzerland, 2018; pp. 1–7. [CrossRef]
40. Cencini, C. Physical process and human activities in the evolution of Po River delta, Italy. *J. Coast. Res.* **1998**, *14*, 774–793.
41. Gabbianelli, G.; Del Grande, C.; Simeoni, U.; Zamariolo, A.; Calderoni, G. Evoluzione dell'area di Goro negli ultimi cinque secoli (Delta del Po). *Studi Costieri* **2000**, *2*, 45–63.
42. Simeoni, U.; Fontolan, G.; Tessari, U.; Corbau, C. Domains of spit evolution in the Goro area, Po River delta, Italy. *Geomorphology* **2007**, *86*, 332–348. [CrossRef]
43. Simeoni, U.; Fontolan, G.; Dal Cin, R.; Calderoni, G.; Zamariolo, A. Dinamica sedimentaria dell'area di Goro (Delta del Po). *Studi Costieri* **2000**, *2*, 139–151.
44. Simeoni, U.; Dal Cin, R.; Fontolan, G.; Tessari, U. Morfogenesi ed evoluzione dello Scanno di Goro (Delta del Po). *Studi Costieri* **2000**, *2*, 5–20.
45. Guilcher, A. Angola. In *Encyclopedia of the World's Coastal Landforms*; Bird, E.C.F., Ed.; Springer: Dordrecht, The Netherlands, 2010; pp. 963–967. [CrossRef]
46. Bird, E.C.F. (Ed.) New Brunswick and Nova Scotia. In *Encyclopedia of the World's Coastal Landforms*; Springer: Dordrecht, The Netherlands, 2010; pp. 141–154.
47. Zimmermann, M.; Prescott, M.M. False Pass, Alaska: Significant changes in depth and shoreline in the historic time period. *Fish. Oceanogr.* **2021**, *30*, 264–279. [CrossRef]
48. Gad, F.K.; Hatiris, G.A.; Loukaidi, V.; Dimitriadou, S.; Drakopoulou, P.; Sioulas, A.; Kapsimalis, V. Long-term shoreline displacements and coastal morphodynamic pattern of north Rhodes Island, Greece. *Water* **2018**, *10*, 849. [CrossRef]
49. Moghaddam, E.I.; Allahdadi, M.N.; Ashrafi, A.; Chaichitehrani, N. Coastal system evolution along the southern Caspian Sea coast using satellite image analysis: Response to the sea level fall during 1994-2-15. *Arab. J. Geosci.* **2021**, *14*, 771. [CrossRef]
50. Jose, F.; Carlin, F. Storm-Driven Morphodynamics of a Sandy Beach in Florida. *J. Coast. Res.* **2022**, *38*, 896–907. [CrossRef]
51. Taveneau, A.; Almar, R.; Bergsma, E.W.; Sy, B.A.; Ndour, A.; Sadio, M.; Garlan, T. Observing and predicting coastal erosion at the Langue de Barbarie sand spit around Saint Louis (Senegal, West Africa) through satellite-derived digital elevation model and shoreline. *Remote Sen.* **2021**, *13*, 2454. [CrossRef]
52. Google Earth Pro. 2023. Available online: http://www.earth.google.com (accessed on 11 April 2023).
53. Harvey, N.; Gross, A.M.; Jose, F.; Savarese, M.; Missimer, T. Geomorphologic impact of Hurricane Irma on Marco Island, southwest Florida. *Nat. Hazards* **2021**, *3*, 1–17. [CrossRef]
54. Navionic ChartViewer. 2023. Available online: https://webapp.navionics.com (accessed on 11 April 2023).
55. Maicu, F.; Alessandri, J.; Pinardi, N.; Verri, G.; Umgiesser, G.; Lovo, S.; Turolla, S.; Paccagnella, T.; Valentini, A. Downscaling with an unstructured coastal-ocean model to the Goro Lagoon and the Po River delta branches. *Front. Mar. Sci.* **2021**, *8*, 647781. [CrossRef]
56. Smith, W.H.F.; Sandwell, D.T. Global sea floor topography from satellite altimetry and ship depth soundings. *Science* **1997**, *277*, 1956–1962. [CrossRef]
57. Hersbach, H.; Bell, B.; Berrisford, P.; Biavati, G.; Horányi, A.; Muñoz Sabater, J.; Nicolas, J.; Peubey, C.; Radu, R.; Rozum, I.; et al. *ERA5 Hourly Data on Single Levels from 1940 to Present*; Copernicus Climate Change Service (C3S) Climate Data Store (CDS): Reading, UK, 2023. [CrossRef]

58. Pe'eri, S.; Keown, P.; Snyder, L.P.; Gonsalves, M.; Nyberg, J. Reconnaissance surveying of Bechevin Bay, AK using satellite-derived bathymetry. In Proceedings of the US Hydrographic Conference 2015, National Harbor, MD, USA, 16–19 March 2015.
59. Flater, D. WXTide32. 2007. Available online: http://www.wxtide32.com (accessed on 11 April 2023).
60. Canadian Hydrographic Service. 2023. Available online: https://tides.gc.ca/en/stations (accessed on 11 April 2023).
61. Davies, J.L. A morphogenetic approach to world shorelines. *Z. Geomorphol.* **1964**, *8*, 1–42.
62. Woodroffe, C.D. *Coasts: Form, Process and Evolution*; Cambridge University Press: Cambridge, UK, 2003; 640p.
63. *GloVis*; 2023. Available online: http://glovis.usgs.gov (accessed on 11 April 2023).
64. Alcántara-Carrió, J.; Fontán Bouzas, A.; Albarracín, S.; Correa, I.D.; Montoya Montes, I.; Mahiques, M. Geomorphological coastal classification after natural processes and human disturbance. *Oceanography* **2014**, *2*, e108. [CrossRef]
65. Petersen, D.; Deigaard, R.; Fredsøe, J. Modelling the morphology of sandy spits. *Coast. Eng.* **2008**, *55*, 671–684. [CrossRef]
66. Kim, D.; Jo, J.; Nam, S.I.; Choi, K. Morphodynamic evolution of paraglacial spit complexes on a tide-influenced Arctic fjord delta (Dicksonfjorden, Svalbard). *Mar. Geol.* **2022**, *447*, 106800. [CrossRef]
67. Carr, A.P. Aspects of spit development and decay: The estuary of the River Ore, Suffolk. *Field Stud.* **1972**, *3*, 633–653.
68. Carr, A.P. The estuary of the river Ore, Suffolk: Three decades of change in a longer-term context. *Field Stud.* **1986**, *6*, 439–458.
69. Fox, D.; Pontee, N.I.; Fisher, E.; Box, S.; Rogers, J.R.; Reeve, D.E.; Chadwick, A.J.; Sims, P. Spits and flood risk: The Exe estuary. In Proceedings of the Flood and Coastal Management Conference, Manchester, UK, 1–3 July 2008; pp. 1–10.
70. Harlow, D.A. The littoral sediment budget between Selsey Bill and Gilkicker Point, and its relevance to coast protection works on Hayling Island. *Q. J. Eng. Geol. Hydrogeol.* **1979**, *12*, 257–265. [CrossRef]
71. Kidson, C. Dawlish Warren: A study of the evolution of the sand spits across the mouth of the River Exe in Devon. *Trans. Papers Inst. Br. Geogr.* **1950**, *16*, 69–80. [CrossRef]
72. Kidson, C. The growth of sand and shingle spits across estuaries. *Z. Geomorphol.* **1963**, *7*, 1–22.
73. Devoy, R.J.N. The development and management of the Dingle Bay spit-barriers of Southwest Ireland. In *Sand and Gravel Spits*; Randazzo, G., Jackson, D., Cooper, A., Eds.; Coastal Research Library 12; Springer: Cham, Switzerland, 2015; pp. 139–180. [CrossRef]
74. Rodríguez-Ramírez, A.; Morales, J.A.; Delgado, I.; Cantano, M. The impact of man on the morphodynamics of the Huelva coast. *J. Iber. Geol.* **2008**, *34*, 313–327.
75. Robinson, A.H.W. The harbor entrances of Poole, Christchurch and Pagham. *Geog. J.* **1955**, *121*, 33–50. [CrossRef]
76. Levoy, F.; Monfort, O.; Anthony, E.J. Multi-decadal mobility of a managed sandy tidal coast (Normandy, France): Behavioural variability in a context of sea-level rise and increasing storm intensity. *Reg. Stud. Mar. Sci.* **2023**, *62*, 102973. [CrossRef]
77. Boyd, R.; Dalrymple, R.W.; Zaitlin, B.A. Classification of coastal sedimentary environments. *Sedim. Geol.* **1992**, *80*, 139–150. [CrossRef]
78. Ciavola, P.; Corbau, C.; Cibin, U.; Perini, L. Mapping of the coastal zone of the Emilia-Romagna region using geographical information systems. In Proceedings of the Sixth International Conference on the Mediterranean Coastal Environment, Ravenna, Italy, 7–11 October 2003; Volume 3, pp. 2363–2374.
79. Short, A.D. Beach dynamics and nearshore morphology of the Alaskan Arctic coast, 2498. In *LSU Historical Dissertations and Theses*; Louisiana State University and Agricultural & Mechanical College: Baton Rouge, LA, USA, 1973; 140p. Available online: https://digitalcommons.lsu.edu/gradschool_disstheses/2498 (accessed on 20 March 2023).
80. Anthony, E.J.; Marriner, N.; Morhange, C. Human influence and the changing geomorphology of Mediterranean deltas and coasts over the last 6000 years: From progradation to destruction phase? *Earth Sci. Rev.* **2014**, *139*, 336–361. [CrossRef]
81. Coleman, J.M.; Gagliano, S.M. Cyclic sedimentation in the Mississippi river deltaic plain. *Gulf Coast Ass. Geol. Societ. Trans.* **1964**, *14*, 67–80.
82. Wu, X.; Bi, N.; Kanai, Y.; Saito, Y.; Zhang, Y.; Yang, Z.; Fan, D.; Wang, H. Sedimentary records off the modern Huanghe (Yellow River) delta and their response to deltaic river channel shifts over the last 200 years. *J. Asian Earth Sci.* **2015**, *108*, 68–80. [CrossRef]
83. Elliott, T. Interdistributary bay sequences and their genesis. *Sedimentology* **1974**, *21*, 611–622. [CrossRef]
84. Tye, R.S.; Kosters, E.C. Styles of interdistributary basin sedimentation: Mississippi delta plain, Louisiana. *Trans. Gulf Coast Assoc. Geol. Soc.* **1986**, *36*, 575–588.
85. Coleman, J.M. Dynamic changes and processes in the Mississippi River delta. *Geol. Soc. Am. Bull.* **1988**, *100*, 999–1015. [CrossRef]
86. Overduin, P.P.; Strzelecki, M.C.; Grigoriev, M.N.; Couture, N.; Lantuit, H.; St-Hilaire-Gravel, D.; Günther, F.; Wetterich, S. Coastal changes in the Arctic. *Geol. Soc. Lond. Spec. Publ.* **2014**, *388*, 103–129. [CrossRef]
87. Héquette, A.; Ruz, M.H. Spit and barrier islands migration in the southeastern Canadian Beafourt Sea. *J. Coast. Res.* **1991**, *7*, 677–698.
88. Gibbs, A.E.; Richmond, B.M. *National Assessment of Shoreline Change: Historical Shoreline Change along the North Coast of Alaska, US–Canadian Border to Icy Cape*; US Department of the Interior, US Geological Survey: Washington, DC, USA, 2015; 110p.
89. Xue, P.; Chen, C.; Beardsley, R.C.; Limeburner, R. Observing system simulation experiments with ensemble Kalman filters in Nantucket Sound, Massachusetts. *J. Geophys. Res. Oceans* **2011**, *116*, C01011. [CrossRef]
90. Piller, W.E.; Pervesler, P.; Golebiowski, R.; Kleemann, K.; Mansour, A.; Rupp, C. The northern Bay of Safaga (Red Sea, Egypt): An actuopalaeontological approach. 1. Topography and bottom facies. *Beitr. Paläont. Österr* **1989**, *15*, 103–147.

91. Marriner, N.; Goiran, J.P.; Morhange, C. Alexander the Great's tombolos at Tyre and Alexandria, eastern Mediterranean. *Geomorphology* **2008**, *100*, 377–400. [CrossRef]
92. Héquette, A.; Ruz, M.H.; Hill, P.R. The effects of the Holocene sea level rise on the evolution of the southeastern coast of the Canadian Beaufort Sea. *J. Coast. Res.* **1995**, *11*, 494–507.
93. Ward, R.D. Sedimentary response of Arctic coastal wetlands to sea level rise. *Geomorphology* **2020**, *370*, 107400. [CrossRef]
94. Da Lio, C.; Tosi, L. Vulnerability to relative sea-level rise in the Po River delta (Italy). *Estuar. Coast. Shelf Sci.* **2019**, *228*, 106379. [CrossRef]
95. Hammar-Klose, E.S.; Pendleton, E.A.; Thieler, E.R.; Williams, S.J.; Norton, G.A. *Coastal Vulnerability Assessment of Cape Cod National Seashore (CACO) to Sea-Level Rise*; Open File Report, 02-233; US Geological Survey: Reston, VA, USA, 2003; 18p.
96. Orford, J.D.; Carter, R.W.G.; Jennings, S.C. Control domains and morphological phases in gravel-dominated coastal barriers of Nova Scotia. *J. Coast. Res.* **1996**, *12*, 589–604.
97. Nienhuis, J.H.; Ashton, A.D.; Nardin, W.; Fagherazzi, S.; Giosan, L. Alongshore sediment bypassing as a control on river mouth morphodynamics. *J. Geophys. Res. Earth Surf.* **2016**, *121*, 664–683. [CrossRef]
98. Bezzi, A.; Casagrande, G.; Martinucci, D.; Pillon, S.; Del Grande, C.; Fontolan, G. Modern sedimentary facies in a progradational barrier-spit system: Goro lagoon, Po River delta, Italy. *Estuar. Coast. Shelf Sci.* **2019**, *227*, 106323. [CrossRef]
99. Maicu, F.; De Pascalis, F.; Ferrarin, C.; Umgiesser, G. Hydrodynamics of the Po river-delta-sea system. *J. Geophys. Res. Oceans* **2018**, *123*, 6349–6372. [CrossRef]
100. Bezzi, A.; Pillon, S.; Popesso, C.; Casagrande, G.; Da Lio, C.; Martinucci, D.; Tosi, L.; Fontolan, G. From rapid coastal collapse to slow sedimentary recovery: The morphological ups and downs of the modern Po River delta. *Estuar. Coast. Shelf Sci.* **2021**, *260*, 107499. [CrossRef]
101. Penland, S.; Boyd, R.; Suter, J.R. Transgressive depositional systems of the Mississippi Delta Plain: A model for barrier shoreline and shelf sand development. *J. Sediment. Petrol.* **1988**, *58*, 932–949.
102. Corbau, C.; Simeoni, U.; Zoccarato, C.; Mantovani, G.; Teatini, P. Coupling land use evolution and subsidence in the Po River delta, Italy: Revising the past occurrence and prospecting the future management challenges. *Sci. Total Environ.* **2019**, *654*, 1196–1208. [CrossRef]
103. Black, K.P.; Andrews, C.J. Sandy shoreline response to offshore obstacles Part 1: Salient and tombolo geometry and shape. *J. Coast. Res.* **2001**, *29*, 82–93.
104. Davies, J.L. *Geographical Variation in Coastal Development*; Longman: London, UK; New York, NY, USA, 1980; 212p.
105. Dally, W.R.; Pope, J. *Detached Breakwaters for Shore Protection*; Technical Report CERC-86-1; U.S. Army Corps of Engineers, Coastal Engineering Research Center, Waterways Experiment Station: Vicksburg, MS, USA, 1986; 62p.
106. Van Rijn, L.C. Coastal erosion and control. *Ocean Coast. Manag.* **2011**, *54*, 867–887. [CrossRef]
107. Alcántara-Carrió, J.; Sasaki, D.; Mahiques, M.; Taborda, R.; Souza, L.A.P. Sedimentary constraints on the development of a narrow deep strait (São Sebastião Channel, SE Brazil). *Geo-Mar. Lett.* **2017**, *37*, 475–488. [CrossRef]
108. Gourlay, M.R. Beach processes in the vicinity of offshore breakwaters. In Proceedings of the 5th Australasian Conference on Coastal and Ocean Engineering, Perth, Australia, 25–27 November 1981; pp. 132–137.
109. Sterr, H. Comparative studies of coastal erosion in the FRG. *J. Coast. Res.* **1990**, *Sp.I. 9*, 821–837.
110. Hofstede, J. Coastal flood defense and coastal protection along the Baltic Sea coast of Schleswig-Holstein. *Die Küste Arch. Res. Technol. North Sea Balt. Coast* **2008**, *74*, 170–178.
111. Giese, G.S.; Borrelli, M.; Mague, S.T. Tidal inlet evolution and impacts of anthropogenic alteration: An example from Nauset Beach and Pleasant Bay, Cape Cod, Massachusetts. *Northeastern Nat.* **2020**, *27* (Suppl. S10), 1–21. [CrossRef]
112. Stéphan, P.; Suanez, S.S.; Fichaut, B. Long-term morphodynamic evolution of the Sillon de Talbert gravel barrier (Brittany, France). *Shore Beach* **2012**, *80*, 19–36.
113. Vespremeanu-Stroe, A.; Preoteasa, L. Morphology and the cyclic evolution of Danube delta spits. In *Sand and Gravel Spits*; Randazzo, G., Jackson, D., Cooper, A., Eds.; Coastal Research Library 12; Springer: Cham, Switzerland, 2015; pp. 327–339.
114. Nuyts, S.; O'Shea, M.; Murphy, J. Monitoring the Morphodynamic Cannibalization of the Rossbeigh Coastal Barrier and Dune System over a 19-Year Period (2001–2019). *J. Mar. Sci. Eng.* **2020**, *8*, 421. [CrossRef]
115. Aubrey, D.G.; Speer, P.E. Updrift migration of tidal Inlets. *J. Geol.* **1984**, *92*, 531–545. [CrossRef]
116. Peterson, C.D.; Murillo-Jiménez, J.M.; Stock, E.; Price, D.M.; Hostetler, S.W.; Percy, D. Origins of late-Pleistocene coastal dune sheets, Magdalena and Guerrero Negro, from continental shelf low-stand supply (70–20 ka), under conditions of southeast littoral-and eolian-sand transport, in Baja California Sur, Mexico. *Aeolian Res.* **2017**, *28*, 13–28. [CrossRef]
117. Murillo de Nava, J.M.; Gorsline, D.S. Holocene and modern dune morphology for the Magdalena coastal plain and islands, Baja California Sur, Mexico. *J. Coast. Res.* **2000**, *16*, 915–925.
118. Bruun, P.; Mehta, A.; Jonsson, I.G. *Stability of Tidal Inlets: Theory and Engineering*; Developments in Geotechnical Engineering; Elsevier: Amsterdam, The Netherlands, 1978; Volume 23, 510p.
119. Nienhuis, J.H.; Ashton, A.D. Mechanics and rates of tidal inlet migration: Modeling and application to natural examples. *J. Geophys. Res. Earth Surf.* **2016**, *121*, 2118–2139. [CrossRef]
120. Lynch-Blosse, M.A.; Kumar, N. Evolution of downdrift-offset tidal inlets: A model based on the Brigantine Inlet system of New Jersey. *J. Geol.* **1976**, *84*, 165–178. [CrossRef]

121. Qi, Y.; Yu, Q.; Gao, S.; Li, Z.; Fang, X.; Guo, Y. Morphological evolution of river mouth spits: Wave effects and self-organization patterns. *Estuar. Coast. Shelf Sci.* **2021**, *262*, 107567. [CrossRef]
122. Chi, S.; Zhang, C.; Wang, P.; Shi, J.; Li, F.; Li, Y.; Wang, P.; Zheng, J.; Sun, J.; Nguyen, V.T. Morphological evolution of paired sand spits at the Fudu river mouth: Wave effects and anthropogenic factors. *Mar. Geol.* **2023**, *456*, 106991. [CrossRef]
123. Leatherman, S.P. Reworking of glacial outwash sediments along outer Cape Cod: Development of Provincetown spit. In *Glaciated Coasts*; FitzGerald, D.M., Roshan, P.S., Eds.; Academic: London, UK, 1987; pp. 447–464.
124. Leatherman, S.P.; Zaremba, R.E. Dynamics of a northern barrier beach: Nauset Spit, Cape Cod, Massachusetts. *Geol. Soc. Am. Bull.* **1986**, *97*, 116–124. [CrossRef]
125. Giese, G.S.; Adams, M.B.; Rogers, S.S.; Dingman, S.L.; Borrelli, M.; Smith, T.L. Coastal Sediment Transport on outer Cape Cod Massachusetts: Observations and Theory. In Proceedings of the Coastal Sediments, Miami, FL, USA, 2–6 May 2011; Rosati, J.D., Wang, P., Roberts, T.M., Eds.; World Scientific Pub Co Inc.: Miami, FL, USA, 2011; pp. 2353–2365.
126. Borrelli, M.; Giese, G.S.; Mague, S.T.; Smith, T.L.; Mittermayer, A.; Legare, B.J.; Solazzo, D. *Potential Impacts to the Nauset Barrier from the Proposed Dredging and Disposal in Nauset Harbor. A Technical Report prepared for the Town of Eastham*; Tech Rep: 19-CL07; Center for Coastal Studies: Provincetown, MA, USA, 2019; 19p.
127. Giese, G.S.; Aubrey, D.G.; Liu, J.T. *Development, Characteristics, and Effects of the New Chatham Harbor Inlet*; Woods Hole Oceanographic Institution: Woods Hole, MS, USA, 1989; 33p.
128. FitzGerald, D.M.; Pendleton, E. Inlet formation and evolution of the sediment bypassing system: New Inlet, Cape Cod, Massachusetts. *J. Coast. Res.* **2002**, *36*, 290–299. [CrossRef]
129. Borrelli, M.; Oakley, B.A.; Giese, G.S.; Boothroyd, J.C. Inlet formation as a result off hydraulic inefficiency leading to further inlet instability. In Proceedings of the Coastal Sediments, Miami, FL, USA, 2–6 May 2011; pp. 519–532.
130. Berman, G. *Longshore Sediment Transport Cape Cod Massachusetts*; Woods Hole Oceanographic Institute & Cape Cod Cooperative Extension: Woods Hole, MS, USA, 2011; 47p.
131. NASA. Coastline Change. NASA Earth Observatory. 2020. Available online: https://earthobservatory.nasa.gov/world-of-change/CapeCod (accessed on 11 April 2023).
132. Giese, G.S.; Mague, S.T.; Rogers, S.S. *A Geomorphological Analysis of Nauset Beach/Pleasant Bay/Chatham Harbor for the Purpose of Estimating Future Configurations and Conditions*; Prepared for the Pleasant Bay Resource Management Alliance; Pleasant Bay Alliance: Harwich, MA, USA, 2009; 32p.
133. Oldale, R.N.; Friedman, J.D.; Williams, R.S. *Changes in Coastal Morphology of Monomoy Island, Cape Cod, Massachusetts U.S. Geological Survey Prof. Paper 750*; U.S. Geological Survey: Reston, VA, USA, 1971; Chapter B; pp. 101–107.
134. Bird, E.C.F. (Ed.) Heidelberg. In *Encyclopedia of the World's Coastal Landforms*; Springer: Dordrecht, The Netherlands, 2010; pp. 641–644.
135. Serizawa, M.; Uda, T.; Miyahara, S. Prediction of formation of recurved sand spit using BG model. In Proceedings of the 36th Coastal Engineering Conference, Baltimore, MD, USA, 30 July–3 August 2018; Volume 36, p. 24.
136. Liu, H. Dynamic changes of coastal morphology following the 2011 Tohoku tsunami. In Proceedings of the 7th International Conference on Asian and Pacific Coasts, Bali, Indonesia, 24–26 September 2013; pp. 594–601.
137. Ruiz, F.; Rodríguez-Vidal, J.; Abad, M.; Cáceres, L.M.; Carretero, M.I.; Pozo, M.; Rodríguez-Llanes, J.M.; Gómez-Toscano, F.; Izquierdo, T.; Font, E.; et al. Sedimentological and geomorphological imprints of Holocene tsunamis in southwestern Spain: An approach to establish the recurrence period. *Geomorphology* **2013**, *203*, 97–104. [CrossRef]
138. Wright, L.D.; Short, A.D. Morphodynamic variability of surf zones and beaches: A synthesis. *Mar. Geol.* **1984**, *56*, 93–118. [CrossRef]
139. Zăinescu, F.I.; Vespremeanu-Stroe, A.; Tătui, F. The formation and closure of the Big Breach of Sacalin spit associated with extreme shoreline retreat and shoreface erosion. *Earth Surf. Process. Landf.* **2019**, *44*, 2268–2284. [CrossRef]
140. Koiwa, N.; Takahashi, M.; Sugisawa, S.; Ito, A.; Matsumoto, H.A.; Tanavud, C.; Goto, K. Barrier spit recovery following the 2004 Indian Ocean tsunami at Pakarang Cape, southwest Thailand. *Geomorphology* **2018**, *306*, 314–324. [CrossRef]
141. Panin, N. The Danube Delta. Geomorphology and Holocene Evolution: A Synthesis. *Geomorphol. Relief Process. Environ.* **2003**, *9*, 247–262. [CrossRef]
142. Preoteasa, L.; Vespremeanu-Stroe, A.; Hanganu, D.; Katona, O.; Timar-Gabor, A. Coastal changes from open coast to present lagoon system in Histria region (Danube Delta). *J. Coast. Res.* **2013**, *65* (Suppl. S1), 564–569. [CrossRef]
143. Frihy, O.; Lawrence, D. Evolution of the modern Nile delta promontories: Development of accretional features during shoreline retreat. *Environ. Geol.* **2004**, *46*, 914–931. [CrossRef]
144. Kelman, D. Strait of Canso transmission line. In *Archaeological Screening & Reconnaissance Antigonish & Inverness Counties, Nova Scotia*; Final Report; Kelman Heritage Consulting: West LaHave, NS, Canada, 2015; 29p.
145. Elliott, E.L. Sandspit of the Otago coast. *N. Z. Geogr.* **1958**, *14*, 65–74. [CrossRef]
146. Canning, P.; Fox, D.; Pontee, N. The benefits of managing spit evolution: A case study in the Exe Estuary, UK. In *Innovative Coastal Zone Management: Sustainable Engineering for a Dynamic Coast*; Cooper, N.J., Ed.; ICE Publishing: London, UK, 2012; pp. 625–635.
147. Karunarathna, H.; Reeve, D.E.; Fox, D.; Box, S.; Pontee, N.; Chadwick, A.; Lawrence, J. Appraising spit dynamics and estuary responses: A coastal management study from the Exe Estuary, UK. In Proceedings of the 31st Coastal Engineering Conference, Hamburg, Germany, 31 August–5 September 2008; World Scientific Publishing Company: Singapore, 2009; pp. 4202–4213. [CrossRef]

148. Johnston, T.W. Sediment Supply, Sediment Transport and Long-Term Shoreline Evolution on "Open" and "Closed" Cellular Coasts: Co. Wexford and Co. Donegal, Ireland. Ph.D. Thesis, The New University of Ulster, Coleraine, Northern Ireland, UK, 1984; 348p.
149. Ruz, M.H. Impact des amenagernents sur l'evolution du littoral de Wexford, sud-est de l´Irlande. *Norois* **1987**, *34*, 261–273. [CrossRef]
150. Anthony, E.J. Patterns of sand spit development and their management implications on deltaic, drift-Aligned coasts: The cases of the Senegal and Volta River delta spits, West Africa. In *Sand and Gravel Spits*; Randazzo, G., Jackson, D., Cooper, A., Eds.; Coastal Research Library 12; Springer: Cham, Switzerland, 2015; pp. 21–36. [CrossRef]
151. Orejarena Rondón, A.F.; Afanador Franco, F.; Ramos de la Hoz, I.; Conde Frías, M.; Restrepo López, J.C. Evolución morfológica de la espiga de Galerazamba, Caribe colombiano. *Bol. Cientif. CIOH* **2015**, *33*, 123–144. [CrossRef]
152. Silva, M.S.; Guedes, C.C.F.; Silva, G.A.M.; Ribeiro, G.P. Active mechanisms controlling morphodynamics of a coastal barrier: Ilha Comprida, Brazil. *Ocean Coast. Res.* **2021**, *69*, 21004. [CrossRef]
153. Lawson, S.K.; Tanaka, H.; Udo, K.; Hiep, N.T.; Tinh, N.X. Morphodynamics and evolution of estuarine sandspits along the bight of Benin coast, West Africa. *Water* **2021**, *13*, 2977. [CrossRef]
154. Restrepo, J.D.; Kjerfve, B.; Correa, I.D.; González, J. Morphodynamics of a high discharge tropical delta, San Juan River, Pacific coast of Colombia. *Mar. Geol.* **2002**, *192*, 355–381. [CrossRef]
155. Villate, D.A.; Portz, L.; Manzolli, R.P.; Alcántara-Carrió, J. Human disturbances of shoreline morphodynamics and dune ecosystem at the Puerto Velero spit (Colombian Caribbean). *J. Coast. Res.* **2020**, *95*, 711–716. [CrossRef]
156. Castillo, M.; Muñoz-Salinas, E.; Sanderson, D.C.W.; Cresswell, A. Landscape evolution of Punta Arena sand spit (SE Baja California Peninsula, NW Mexico): Implications of ENSO on landscape erosion rates. *Catena* **2020**, *193*, 104601. [CrossRef]
157. Nahon, A.; Idier, D.; Senechal, N.; Féniès, H.; Mallet, C.; Mugica, J. Imprints of wave climate and mean sea level variations in the dynamics of a coastal spit over the last 250 years: Cap Ferret, SW France. *Earth Surf. Process. Landf.* **2019**, *44*, 2112–2125. [CrossRef]
158. Orviku, K.; Jaagus, J.; Kont, A.; Ratas, U.; Rivis, R. Increasing activity of coastal processes associated with climate change in Estonia. *J. Coast. Res.* **2003**, *19*, 364–375.
159. Łabuz, T.A. Environmental impacts—Coastal erosion and coastline changes. In *Second Assessment of Climate Change for the Baltic Sea Basin*; The BACC II Team, Ed.; Springer: Cham, Switzerland, 2015; pp. 381–396.
160. Iskander, M.M. Stability of the Northern coast of Egypt under the effect of urbanization and climate change. *Water Sci.* **2021**, *35*, 1–10. [CrossRef]
161. Ogorodov, S.A.; Baranskaya, A.V.; Belova, N.G.; Kamalov, A.M.; Kuznetsov, D.E.; Overduin, P.P.; Shabanova, N.N.; Vergun, A.P. Coastal dynamics of the Pechora and Kara Seas under changing climatic conditions and human disturbances. *Geogr. Environ. Sustain.* **2016**, *9*, 53–73. [CrossRef]
162. Nordstrom, K.F.; Jackson, N.L. Removing shore protection structures to facilitate migration of landforms and habitats on the bayside of a barrier spit. *Geomorphology* **2013**, *199*, 179–191. [CrossRef]
163. Correa, I.D.; Alcántara-Carrió, J.; González, R.D.A. Historical and recent shore erosion along the Colombian Caribbean coast. *J. Coast. Res.* **2005**, *Sp.I. 49*, 52–57.
164. Orford, J. Alternative interpretations of man-induced shoreline changes in Rosslare Bay, southeast Ireland. *Trans. Inst. Br. Geogr.* **1988**, *13*, 65. [CrossRef]
165. Zweers, S. A Study of the Erosion Problem along Rosslare Strand. Master's Thesis, Delft University of Technology, Delft, The Netherlands, 2008; 149p.
166. Simeoni, U.; Corbau, C. A review of the Delta Po evolution (Italy) related to climatic changes and human impacts. *Geomorphology* **2009**, *107*, 64–71. [CrossRef]
167. Stefani, M. The Po River delta region: Depositional evolution, climate change and human Intervention through the last 5000 years. In *Landscapes and Landforms of Italy*; World Geomorphological Landscapes, Soldati, M., Marchetti, M., Eds.; Springer: Cham, Switzerland, 2017; pp. 193–202. [CrossRef]
168. Corbau, C.; Zambello, E.; Nardin, W.; Simeoni, U. Secular diachronic analysis of coastal marshes and lagoons evolution: Study case of the Po River delta (Italy). *Estuar. Coast. Shelf Sci.* **2022**, *268*, 107781. [CrossRef]
169. Vincenzi, A. Coastline Changes in Veneto Region (Italy) from 2012 to 2018 by Means of Multitemporal Orthophotos. Master's Thesis, University of Padua, Padua, Italy, 2022; 118p.
170. Kosyan, R.D.; Krylenko, M.V. Modern state and dynamics of the Sea of Azov coasts. *Estuar. Coast. Shelf Sci.* **2019**, *224*, 314–323. [CrossRef]
171. Hayashi, K.; Hashimoto, K.; Yagisawa, K.; Kobayashi, N. Beach morphologies at Notsukezaki sand spit, Japan. In Proceedings of the 32nd Coastal Engineering Conference, Shanghai, China, 30 June–5 July 2010; p. 2.
172. Itori, S.; Yagisawa, K.; Sasaki, T.; Yanaguchi, R.; Kobayashi, N. Storm-induced erosion on Notsuzezaki sand spit. In Proceedings of the 36th Coastal Engineering Conference, Baltimore, MD, USA, 30 July–3 August 2018; Volume 1, p. 79. [CrossRef]
173. Zenkovich, V.P. *The Shores of the Black and Azov Seas*; Geographical Press: Moscow, Russia, 1958; 374p. (In Russian)
174. Pontee, N.I.; Townend, I.H.; Chesher, T.; McLaren, P. To Breach or not to Breach? Spit dynamics and coastal management. In Proceedings of the Coastal Engineering 2002 Conference: Solving Coastal Conundrums, Cardiff, UK, 7–12 July 2002; Smith, J.K., Ed.; World Scientific Publishing Co. Pte. Ltd.: Cardiff, Wales, UK, 2003; pp. 3799–3811.

175. Stéphan, P.; Suanez, S.; Fichaut, B.; Autret, R.; Blaise, E.; Houron, J.; Ammann, J.; Grandjean, P. Monitoring the medium-term retreat of a gravel spit barrier and management strategies, Sillon de Talbert (North Brittany, France). *Ocean Coast. Manag.* **2018**, *158*, 64–82. ISSN 0964-5691. [CrossRef]
176. Vitousek, S.; Buscombe, D.; Vos, K.; Barnard, P.L.; Ritchie, A.C.; Warrick, J.A. The future of coastal monitoring through satellite remote sensing. *Cambridge Prism. Coast. Futur.* **2023**, *1*, e10. [CrossRef]